NATIONAL ADVISORY COMMITTEE FOR AERONAUTICS

TECHNICAL NOTE 3090

INVESTIGATION OF SANDWICH CONSTRUCTION UNDER LATERAL AND AXIAL LOADS

By Wilhelmina D. Kroll, Leonard Mordfin, and William A. Garland

National Bureau of Standards

Washington

December 1953

NATIONAL ADVISORY COMMITTEE FOR AERONAUTICS

TECHNICAL NOTE 3090

INVESTIGATION OF SANDWICH CONSTRUCTION UNDER LATERAL AND AXIAL LOADS

By Wilhelmina D. Kroll, Leonard Mordfin,
and William A. Garland

SUMMARY

Tests under combined axial load and lateral pressure were made on 12 bonded sandwich panels with simply supported loaded edges and free unloaded edges. The panels were nominally 30 inches long, 17 inches wide, and 1/2 or 3/4 inch thick. The sheets were 75S-T6 alclad aluminum alloy, 0.025 or 0.032 inch thick. The core was a hexagonal honeycomb of 0.005-inch 2S-H18 aluminum foil.

The maximum load and the mode of failure were observed for all the panels. Lateral deflections and axial strains were also measured.

Based on previous work by Hoff and Mautner in determining the buckling load of sandwich columns, equilibrium equations for a sandwich column with simply supported ends under combined axial load and lateral pressure were derived and, from them, the formulas for axial strain and lateral deflection.

Comparison of computed values of lateral deflection and axial strain with experimental values showed that, in most cases, the theory was conservative in predicting larger strains or deflections than those measured. This discrepancy is attributed to the fact that the sandwich column theory does not take into account the anticlastic bending which was observed in the panel tests.

Methods of computing the failing loads of the panels are presented. Agreement between computed maximum loads and the experimental failing loads is within 9 percent.

INTRODUCTION

Sandwich panels are finding increasing use in aircraft structures where a high strength-weight ratio is a desirable characteristic. When

comparing panels of equal weight, a sandwich panel will have a higher strength-weight ratio in bending than a solid panel of the same length and width because of its larger moment of inertia. Because of the low effective shear moduli of materials used in the core, however, the effect of shear must be considered in the computation of lateral deflections of sandwich panels and of their column strengths.

Many of the component parts of airplanes in which sandwich construction is used are subjected to lateral pressure and axial load simultaneously. The tests described in this paper were made, therefore, to determine the strength of sandwich panels of various thicknesses under these combined loads and to compare the results with values computed from the theory presented herein for sandwich construction, based on the work of Hoff and Mautner (ref. 1).

The panels and coupons of the materials used in their construction were fabricated by The Glenn L. Martin Co.

Except for shear tests on coupons made at the Forest Products Laboratory, this investigation was conducted at the National Bureau of Standards under the sponsorship and with the financial assistance of the National Advisory Committee for Aeronautics. The authors acknowledge the excellent cooperation of the Forest Products Laboratory.

DESCRIPTION OF PANELS

Components and Dimensions

Each of the 12 panels was composed of two sheets of 75S-T6 alclad aluminum alloy 0.025 or 0.032 inch thick, separated by a honeycomb core of 0.005-inch 2S-H18 aluminum foil. The core was constructed of individual perforated strips in corrugated form such that, when assembled, they formed an interlocking pattern of regular hexagons, each nominally 3/8 inch across corners. The corrugated strips were bonded together, and the core as a whole was bonded to the sheets with a special adhesive developed by The Glenn L. Martin Co. The individual strips forming the core were placed parallel to the long dimension of the panels. The direction of rolling of the sheets was also along this axis. A panel of this type is shown in figure 1, with one of the sheets partially removed to show the core.

The panels were nominally 30 inches long, 17 inches wide, and 1/2 or 3/4 inch thick. The weight of the core was 6.54 lb/cu ft. The exact dimensions and weights of the panels are given in table 1.

Mechanical Properties

Tensile and compressive tests were performed on specimens of the cover sheet material in the direction of rolling. Representative stress-strain curves are shown in figure 2, and the average mechanical properties in tension and in compression are given in table 2.

Shear tests on six coupons of the sandwich panel material were made by the Forest Products Laboratory using their standard technique described in reference 2. The coupons were 6 inches long, 2 inches wide, and 1/2 inch thick including the cover sheets of 0.032-inch aluminum-alloy sheet. Three of the specimens were loaded parallel to the direction of the core strips and three were loaded perpendicular to this direction. Using the method of reference 2, a representative stress-strain curve for the core was computed for each direction of loading. The results are shown in figure 3. The resulting mechanical properties of the core in shear are presented in table 3. Figure 4 shows typical failures resulting from these tests. It will be noted that, when loaded parallel to the direction of the core strips, failure occurred in the bonds between the core and the sheets. When the specimen was loaded perpendicular to the core strip direction, failure was due to destruction of the core cell walls.

Nondestructive tests were carried out on the panels to determine their flexural rigidities in pure bending. Figure 5(a) illustrates the test setup which was used. A dial gage, mounted upon a three-legged bridge, was used to measure center deflection with respect to the legs of the bridge. The resulting load-deflection curves are given in figure 5(b), and the slope of these curves W/d was inserted in the relation

$$EI = \frac{Wl_1^2 l_2}{16d}$$

where

W total applied load

l_1 panel length between ends of bridge

l_2 moment arm of load

d deflection at center of bridge

The results thus computed are given in column (2), table 4.

TESTS

Panels A, B, C, E, F, G, I, J, K, and L were tested under combined axial load and lateral pressure. Panel D was tested under axial load only and panel H, under lateral pressure only.

Tests Under Combined Loading

At the start of the investigation, panels were tested in pairs, face to face, with an air bag between them supplying lateral pressure. The ends of the panels were clamped, to approach the condition of fixed end support. This method proved unsuccessful, however, because the clamp, in resisting the end bending moment, induced large local shear stresses in the core. These stresses resulted in premature shear failures at the ends.

In an attempt to alleviate this situation, two panels were clamped together with jigs at approximately their quarter points, so that the slope of their deflection curves at the "fixed" ends would be zero and less shear due to the end clamps would be encountered. This would actually have been the case had the panels tended to deflect symmetrically in opposite directions because of the air bag between them. Unfortunately, the panels deflected in opposite directions only up to loads corresponding to the fixed-end column buckling load and then both panels deflected in the same direction. As a result, the jigs did not serve the purpose for which they were designed and undesirable high shearing forces were once more introduced at the fixed ends.

At this point, it was decided to test the panels singly, with simply supported ends, in the method to be described in the succeeding paragraphs. This method proved satisfactory and all combined-loading tests were made in this manner.

Loading.- Axial load was applied to the simply supported panels by a 120,000-pound-capacity Baldwin-Southwark-Tate-Emery hydraulic testing machine. The unloaded edges of the panels were free; the loaded ends were mounted in knife-edge fixtures (A, fig. 6). These fixtures were free to rotate under load in a pair of V-grooves (B, fig. 6), which were machined into a pair of bearing blocks. A second, larger V-groove (C, fig. 6) was cut into each block to provide room for rotation of the knife-edge fixtures as the panel deflected. The loaded ends of the panels were ground flat and parallel before mounting.

Plaster of paris was cast between the bearing blocks and the heads of the machine to take up any irregularities between them. If the indicated strain distribution at the loaded ends of the panels was not

uniform within ±15 percent at 10 percent of the estimated maximum load, brass and lead foil shims, between 0.0005 and 0.002 inch thick, were inserted between the ground ends of the panel and the knife-edge fixtures (A, fig. 6) until a uniform strain distribution was obtained.

Lateral pressure was applied to one side of the panel (P, fig. 7) by a bellows type of air bag of rubberized cloth (R, figs. 7 and 8). This bag, shown in position in figures 7 and 8, was mounted between the panel and a dummy panel (A, fig. 8). This dummy panel was rigidly attached to the lower bearing block. A roller (B, fig. 8) between the upper portion of this dummy panel and a small stiff plate (C, fig. 8), rigidly attached to the upper bearing block, prevented the dummy panel from receiving more than a negligible amount of the axial load applied by the testing machine (M, figs. 7 and 8).

Air was supplied to the system from a 100-psi air line. It was reduced to the desired pressures and maintained by an Airco pressure regulator in series with a conical seat relief valve having an adjustable blow-off pressure. Pressure was measured with a mercury manometer attached to the output line of the relief valve. The pressure at the manometer was maintained within -0.03 to 0.01 psi in all cases except the test of panel C, in which unforeseen difficulties reduced this precision to 0 to 0.08 psi. The pressure applied to the panel was in greater error as will be discussed subsequently.

By keeping the lateral pressure conservatively low, tipping of the panel end on the knife-edge seat (A, fig. 6) was avoided. The ratio of lateral pressure q to axial load P was always such that

$$\frac{qwL}{P} < \frac{t}{a}\left(\frac{1 - \frac{2a}{t}\tan\frac{d\pi}{L}}{1 + \frac{t}{2a}\tan\frac{d\pi}{L}}\right)$$

where

w panel width

L panel length

t panel thickness

a distance from knife edge to panel end

d panel deflection at midlength

The axial and lateral loads were increased in small steps until the test lateral pressure was reached. With lateral pressure constant, the panel was then tested to failure by further increases in axial load.

Measurements.- Deflections of the panels were measured in both the lateral and axial directions.

Lateral deflection was measured at the nine points on the face of the panel shown in figure 9, using dial gages with a least count of 0.001 inch. The gages were mounted upon a three-legged bridge, shown in figure 7. At loads approaching failure, readings of lateral deflection were not taken for reasons of safety.

Axial deflection, or shortening, was measured at two places near the unloaded edges of the panel. Dial gages (G, figs. 7 and 8) with a least count of 0.001 inch were attached to the upper bearing block. Extension rods (E, figs. 7 and 8) had their upper ends attached to these gages and their lower ends seated in dimpled points in the lower bearing block. Aluminum rods were used to compensate for any thermal expansion and contraction of the panels which might occur during the tests.

Strain was measured with SR-4 wire strain gages, type A-3. Eleven gages were attached to each sheet of panels B, C, E, F, G, I, J, K, and L, in the locations shown in figure 9. The 12 gages attached near the loaded ends of each of these panels were used primarily as a guide in shimming the ends to obtain a uniform strain distribution. Ten gages were mounted across the center of these panels, where maximum strain was expected. On panel A, gages 13, 14, 16, 17, 18, 19, 21, and 22 were omitted, but the other gages were located as shown in figure 9.

Test Under Axial Loading Only

Loading.- Axial loading of panel D, which was tested without lateral pressure, was applied in the same manner as described above for the combined-loading tests. All equipment utilized only for the application of lateral pressure was removed.

Measurements.- Measurements of axial deflection, lateral deflection, and strain were made in the same manner as in the combined-loading tests.

Test Under Lateral Pressure Only

Loading.- Panel H, which was tested under lateral pressure alone, was mounted between the heads of a large testing machine as shown in figure 10.

The panel was supported in a horizontal position by a pair of solid steel cylinders which provided simple end support. These cylinders were rigidly attached to a pair of steel blocks resting on the smooth lubricated flanges of a pair of I-beams which, in turn, rested on the fixed bottom head of the machine. Pressure was applied to the top side of the panel by a rubber air bag bearing upon it. The top head of the machine was fixed at roughly 1 inch above the panel to act as the surface against which the bag was to react. It served the same purpose as the dummy panel in the combined-loading tests.

As the panel deflected, the adjusting screws (fig. 10) were used to move the blocks - and the attached rollers - so that contact between the rollers and the panel was maintained within 1/8 inch of 1/2 inch from the ends of the panel.

The pressure in the bag was controlled and measured with the same equipment used in the combined-loading tests.

Measurements.- Lateral deflection of the panel was measured at the same nine points as in the combined-loading tests (fig. 9). Hooks of thin wire were cemented to the underside of the panel at these points and scales with a least count of 1 millimeter were hung vertically from them. Thin wires, fixed to the I-beams, passed lengthwise across the panel at each of the gage lines (a, b, and c, fig. 11). To facilitate the reading of the scales at their intersections with the wires, three reading telescopes were employed.

Strain was measured with strain gages of the same kind used in the combined-loading tests; the gages were placed at the same locations as the 10 center gages (fig. 9) used in those tests.

Computation of Lateral Pressure

In the combined-loading tests, it was observed that the air bag overlapped the unloaded edges of the panels. This produced an added force on these edges which was computed to be approximately 6 percent of the force exerted on the panels by direct pressure of the bag. (See appendix A for a derivation of this value.) The total force was then divided by the area of the panels to give the average lateral pressure.

Immediately preceding the test of panel I, the cloth air bag developed several leaks which required a constant flow of air from the pressure regulators to the bag to maintain constant pressure. This caused a pressure drop due to pipe friction between the manometer and the air bag. At the end of the tests, this pressure drop was measured for several pressures and was found to be approximately 19 percent of the indicated manometer pressure. For panels I, J, K, and L, the pressure in the air bag was taken, therefore, as 81 percent of the indicated manometer pressure.

A similar pressure drop existed in the lateral-load test as a result of leakage from the rubber air bag used in this test. Unfortunately, an attempt to measure this pressure drop was not made until several months after the lateral-load test and, in the intervening period, the rubber in the bag deteriorated to such an extent that reliable values could not be obtained experimentally. Assuming that the theory for the lateral-load test was correct at low pressures, the pressure drop was determined by making the initial portion of the experimental load-strain curve agree with the theoretical one. To make the curves agree, the pressure in the bag had to be taken as 86 percent of the indicated manometer pressure; this factor was then applied to all of the pressures measured in the lateral-load test. This may account for some of the discrepancy observed between theoretical and experimental results at higher pressures since the air leaks in the rubber bag actually changed somewhat with pressure.

Also in the lateral-load test, it was observed that, as the panel deflected, the bag tended to assume an elliptical cross section and thus did not bear against the full width of the panel. The average pressure on the panel was taken as the pressure in the bag multiplied by the ratio of the loaded panel area to the total panel area. This condition is discussed in more detail in appendix B.

RESULTS OF TESTS

Strain and Lateral Deflection

Figure 11 shows the laterally deflected shape of panel A. This general shape was common to all of the panels; the panels deflected more near their vertical edges than near their vertical center lines.

Load-strain curves of the 10 center strain gages of a representative panel are shown in figure 12. It is evident that the strain becomes more compressive from the edges toward the vertical center line of the panel; this is attributed to anticlastic curvature.

In figure 13 are given the strain and the deflection distributions at the midlength of a typical panel at an axial load of 3,050 pounds and a lateral pressure of 1.58 psi. The percentage difference between edge and center strain reached about 50 percent just before failure in all panels tested under combined loading.

In computing the average strains and deflections of the panels at their transverse center lines, the areas under the corresponding transverse distribution curves (e.g., fig. 13) were integrated and divided by the width of the panel, except for panel A where this was not possible.

For panel A, having gages only at the center of the transverse center line, the data from panels B and C, which had the same dimensions as panel A, were utilized in the following manner. It was observed that for panels B and C the ratio of the average strain to the center strain at the midlength was substantially constant for all axial loads up to those very near failure. For the tensile sheet this ratio was 1.20 ± 0.04 and for the compressive sheet 0.94 ± 0.03. These ratios were then applied to the two center gages of panel A to determine the average strains in panel A.

Figures 14, 15, 16, and 17 are plots of axial load against average strain, each figure depicting the results of tests on panels of a single group. Figures 18, 19, 20, and 21 are each graphs of axial load plotted against average center deflection for panels of a single group. These figures show that, for panels with the same dimensions, an increase in lateral pressure at a given axial load resulted in increased strains and deflections. Furthermore, as expected, a comparison of figures 14 through 21 indicates that, for a given pressure and axial load, panels of higher flexural rigidity have lower strains and deflections.

All data were plotted from the point at which the predetermined lateral pressures were reached. The data for panel C (figs. 14 and 18) are not so consistent as for the others, presumably because difficulties encountered in maintaining constant pressure in this test caused strain and deflection readings to fluctuate.

The mean of the average strains in the tensile and compressive sheets of the panels was compared with values of P/AE, where A is the cross-sectional area of the faces and E is Young's modulus of the faces. Below the elastic limit, the difference was less than 3 percent in almost every case.

In the case of panel D, which was tested with axial load only, both sheets strained in compression until the critical buckling load was approached.

Figures 22 and 23 are graphs of average lateral pressure against average center strain and deflection, respectively, for panel H which was tested under lateral pressure only.

Permanent Set

A measurement of permanent set before failure was made on panel G, considered a representative panel. At 4,300 pounds, or 95 percent of the maximum axial load, both the axial load and the lateral pressure (2.66 psi) were removed. Deflections and strains were then measured.

It was found that a permanent center deflection of about 0.10 inch existed, as well as permanent strains of approximately 50×10^{-6} in the tension sheet and 400×10^{-6} in the compression sheet.

Axial Deflection

A curve of axial load plotted against shortening, or axial deflection, for a representative panel is shown in figure 24.

Failure

Panels tested under combined load and axial load alone, with the exception of panel E, failed because of buckling of the compressed sheet away from the core and breaking of the bond between this sheet and the core. A failure of this type is shown in figure 25. Failure in panel E was due to shearing of the bond between the compressed sheet and the core at about the quarter length of the panel. An examination of this panel after failure showed a scarcity of adhesive in the area where shearing occurred, indicating that the core was improperly bonded to the sheet in this region.

Panel H, tested under lateral pressure only, failed because of shearing of the core and of the bond between the core and the compressed sheet. This failure is also shown in figure 25.

In no case was any buckling of the sheets observed before actual failure.

Maximum Axial Load

Columns (5) and (6) in table 4 give the lateral pressures and axial loads at failure, respectively, for the panels. Since panel E was imperfectly bonded, the maximum axial load is not indicative of the actual strength of a similar properly fabricated panel under the test lateral pressure.

For panels of a single group, it is seen that an increase in lateral pressure resulted in a decrease in the maximum axial load. At a given pressure, either increased sheet thickness or greater core thickness raised the maximum axial load.

THEORETICAL ANALYSIS

In reference 1, Hoff and Mautner developed, with the use of the principle of virtual displacements, a theory for the bending and buckling of sandwich-type elements from a consideration of the strain energy stored in the faces by extension and bending and in the core by shear and by extension perpendicular to the plane of the faces. The strain energy due to shear in the faces and to extension in the core parallel to the faces was disregarded.

It was realized that the panels of the investigation reported herein, having a length-width ratio of 1.78, were plates and should be analyzed as such for best results. Plate theory, however, is much more cumbersome and difficult to apply with free rather than simply supported edge conditions at the unloaded edges. The simpler, though less adequate, column theory was therefore used in correlating the experimental and theoretical results. Formulas were obtained for the lateral deflection and for the axial strains in the cover sheets of a sandwich column with simply supported ends subjected to lateral load and axial compression (fig. 26).

The derivation of these formulas parallels Hoff and Mautner's work (ref. 1) in deriving the equation for buckling stress of a sandwich column under compressive load alone and is given below. Since a few preliminary tests indicated no flattening of the core, this deformation was not considered in the analysis. It is to be noted that the origin of coordinates is taken at the center of the column and that the derivation is for a column of unit width. The expressions for the strain energy due to displacements u and v and for the shear caused by the displacement v are given in reference 1. If the displacement u is taken at the midthickness of the face, the angle of shear caused by it in the core is

$$\gamma_1 = \frac{2u}{b + t} \tag{1}$$

(See appendix C for definitions of symbols.) With the angle of shear γ_2 due to v equal to

$$\gamma_2 = -v' \tag{2}$$

the strain energy of shear is

$$U_{shear} = \frac{Gb}{2}\int_{-L/2}^{L/2} (\gamma_1 + \gamma_2)^2 \, dx$$

$$= \frac{Gb}{2}\int_{-L/2}^{L/2}\left(\frac{2u}{b + t} - v'\right)^2 dx \tag{3}$$

Using the above equation for the strain energy of shear (eq. (3)) and equations for the strain energy of extension and bending from reference 1, the strain energy stored in a sandwich column subjected to lateral pressure and axial load is

$$U = E_f t\int_{-L/2}^{L/2} (u')^2 \, dx + (EI)_f \int_{-L/2}^{L/2} (v'')^2 \, dx + \frac{Gb}{2}\int_{-L/2}^{L/2}\left(\frac{2u}{b + t} - v'\right)^2 dx \tag{4}$$

The potential of the lateral and axial loads is

$$V = -\int_{-L/2}^{L/2} qv \, dx - \sigma t\int_{-L/2}^{L/2} (v')^2 \, dx \tag{5}$$

The equations of equilibrium are derived from the requirement that the first variation of the total potential must vanish, or

$$\delta(U + V) = 0 \tag{6}$$

Applying equation (6) to the sum of equations (4) and (5),

$$\delta(U + V) = \int_{-L/2}^{L/2}\left[E_f t 2u'\delta u' + 2(EI)_f v''\delta v'' + Gb\left(\frac{2u}{b + t} - v'\right)\left(\frac{2\delta u}{b + t} - \delta v'\right) - q\delta v - 2\sigma t v'\delta v'\right] dx$$

$$= 0 \tag{7}$$

For a simply supported column, the end conditions at $x = \pm L/2$ are

$$u' = v'' = \delta v = 0 \tag{8}$$

Integrating equation (7) by parts twice and making use of end conditions, equations (8),

$$-2E_f t\int_{-L/2}^{L/2} u''\delta u\,dx + 2(EI)_f\int_{-L/2}^{L/2} v^{iv}\delta v\,dx + Gb\int_{-L/2}^{L/2}\frac{4u\delta u}{(b+t)^2}\,dx -$$

$$Gb\int_{-L/2}^{L/2} v''\delta v\,dx - \frac{2Gb}{b+t}\int_{-L/2}^{L/2} v'\delta u\,dx + 2Gb\int_{-L/2}^{L/2}\frac{u'\delta v}{b+t}\,dx +$$

$$\int_{-L/2}^{L/2}(-q\delta v + 2\sigma t v''\delta v)\,dx = 0 \tag{9}$$

In this equation, δu and δv are arbitrary functions of x, so the equation will be satisfied identically if

$$-2E_f t u'' + \frac{4Gb}{(b+t)^2}u - \frac{2Gb}{b+t}v' = 0 \tag{10}$$

and

$$2(EI)_f v^{iv} - Gbv'' + \frac{2Gb}{b+t}u' - q + 2\sigma t v'' = 0 \tag{11}$$

or

$$u'' - \frac{Gb}{(EI)_1}u + \frac{Gb}{(EI)_1}y' = 0 \tag{12}$$

and

$$y^{iv} + \frac{2\sigma t - Gb}{2(EI)_f} y'' + \frac{Gb}{2(EI)_f} u' - \frac{q(b + t)}{4(EI)_f} = 0 \tag{13}$$

where

$$\left.\begin{aligned} (EI)_1 &= t(b + t)^2 E_f/2 \\ 2(EI)_f &= t^3 E_f/6 \\ (EI)_b &= (EI)_1 + 2(EI)_f \\ y &= (b + t)v/2 \end{aligned}\right\} \tag{14}$$

The solution of these simultaneous equations is

$$u = A_1 \cosh p_1 x + A_2 \sinh p_1 x + A_3 \cos p_2 x + A_4 \sin p_2 x + A_5 + \frac{q(b + t)}{4\sigma t} x \tag{15}$$

$$y = \frac{1}{p_1}\left[1 - p_1^2 \frac{(EI)_1}{Gb}\right](A_1 \sinh p_1 x + A_2 \cosh p_1 x) + \frac{1}{p_2}\left[1 + p_2^2 \frac{(EI)_1}{Gb}\right](A_3 \sin p_2 x - A_4 \cos p_2 x) + A_5 x + A_6 + \frac{q(b + t)}{4\sigma t} \frac{x^2}{2} \tag{16}$$

where

$$p_1 = \left|\sqrt{\mu + \nu}\right|$$

$$p_2 = \left|\sqrt{\mu - \nu}\right|$$

$$\mu = \frac{1}{2}\left|\sqrt{\beta^2 + 4\gamma^2}\right|$$

$$\nu = \beta/2$$

$$\beta = \frac{Gb(EI)_b - 2\sigma t(EI)_1}{(EI)_1 2(EI)_f}$$

$$\gamma^2 = \frac{Gb(2\sigma t)}{(EI)_1 2(EI)_f}$$

Using the boundary conditions $u' = y = y'' = 0$ at $x = \pm L/2$ and taking into account the fact that deflections must be symmetrical about the center line, one can solve for the unknowns A_1 to A_6. The resulting equations, when these values are substituted into equations (15) and (16), and equation (14) is used to replace y by v, are

$$u = \frac{q(b + t)}{4\sigma t}\left[-\frac{1}{p_1}\left(\frac{p_2^2}{p_1^2 + p_2^2}\right)\frac{\sinh p_1 x}{\cosh p_1\frac{L}{2}} - \frac{1}{p_2}\left(\frac{p_1^2}{p_1^2 + p_2^2}\right)\frac{\sin p_2 x}{\cos p_2\frac{L}{2}} + x\right] \tag{17}$$

$$v = \frac{q}{2\sigma t}\left\{\left[\frac{(EI)_1}{Gb}\frac{p_2^2}{p_2^2 + p_1^2} - \frac{p_2^2/p_1^2}{p_2^2 + p_1^2}\right]\frac{\cosh p_1 x}{\cosh p_1\frac{L}{2}} + \left[\frac{(EI)_1}{Gb}\frac{p_1^2}{p_2^2 + p_1^2} + \frac{p_1^2/p_2^2}{p_1^2 + p_2^2}\right]\frac{\cos p_2 x}{\cos p_2\frac{L}{2}} - \frac{L^2}{8} - \frac{(EI)_b}{2\sigma t} + \frac{x^2}{2}\right\} \tag{18}$$

As in Hoff and Mautner's work, it was assumed that the axial load was carried by the two facings of the sandwich panel. If the panel is stable, the axial load will cause only a uniform axial compression; this is considered the initial state of the panel. The axial strains at the midthickness of the faces are given, therefore, by

$$\epsilon_x = \frac{\sigma_x}{E_f} \pm u'$$

or

$$\epsilon_x = \frac{\sigma_x}{E_f} \pm \frac{q(b + t)}{4\sigma t} \left(- \frac{p_2^2}{p_2^2 + p_1^2} \frac{\cosh p_1 x}{\cosh p_1 \frac{L}{2}} - \right.$$

$$\left. \frac{p_1^2}{p_1^2 + p_2^2} \frac{\cos p_2 x}{\cos p_2 \frac{L}{2}} + 1 \right) \tag{19}$$

The critical buckling load of a simply supported sandwich column whose core modulus, in the direction of the axis of the column, is small enough to justify the assumption that the entire compressive load is carried by the two faces alone is given by equation (12) of reference 1 as

$$P_{cr} = \frac{P_1 \left[P_2 + Gb \left(1 + \frac{P_2}{P_1} \right) \right]}{P_1 + Gb} \tag{20}$$

where

$$P_1 = \pi^2 (EI)_1 / L^2$$

and

$$P_2 = \pi^2 2 (EI)_f / L^2$$

COMPARISON OF EXPERIMENTAL RESULTS WITH THEORY

The lateral deflection at the center of the panels was computed from equation (18) for the panels under combined loading, using average dimensions for panels of a group, and compared with the deflections measured during the tests. The theoretical curves are plotted in figures 18, 19, 20, and 21. The extreme-fiber strains at the center of the panel were measured; for comparison purposes, values of these strains were computed, using average dimensions for the panels of a group, from

$$\epsilon_x = \frac{\sigma_x}{E_f} \pm \frac{q(b + 2t)}{4\sigma t}\left(-\frac{p_2^2}{p_2^2 + p_1^2}\frac{\cosh p_1 x}{\cosh p_1 \frac{L}{2}} - \frac{p_1^2}{p_2^2 + p_1^2}\frac{\cos p_2 x}{\cos p_2 \frac{L}{2}} + 1\right) \tag{21}$$

In using this equation, it was assumed that the strain due to lateral loading, the second term of equation (19), varied linearly from the mid-thickness of the face to the extreme fiber and that the strain due to axial load was uniform throughout the face, leaving the first term the same as in equation (19). The computed values of the strains are plotted in figures 14, 15, 16, and 17.

The experimental values were, in general, lower than those predicted by theory. The maximum discrepancy in strain was 20 percent and existed in the tension sheet of panel G at 4,000 pounds. The maximum difference in lateral deflection was 25 percent and was observed in the test of panel C. These discrepancies appear to be due to anticlastic bending which is not taken into account by the theory. Anticlastic bending produces a transverse curvature in the panel (see fig. 13) which increases its stiffness, or more precisely, the moment of inertia about its neutral plane. This reduces the strains and deflections for a given loading condition. Since the amount of anticlastic curvature present in any test increases with the lateral deflection, it can be expected to decrease in significance with increase in panel stiffness. This was observed in the tests where the effect of anticlastic curvature was greatest for the group I panels and successively smaller for groups II, III, and IV. This explains why the discrepancies between theory and experiment were, in general, greater for the 1/2-inch panels than for the 3/4-inch panels. Furthermore, anticlastic bending is proportional to the bending moment applied to the specimen and therefore increases with increased lateral pressure and axial load. For this reason, within a single group, panels tested at higher pressures showed larger differences. For any given panel, the discrepancy increased with axial load until the elastic limit

was reached, at which time strains and deflections approached, and often exceeded, theoretical values for an elastic panel. In the plastic region, an effective modulus would have to be used if theory and experiment were to be compared.

It is important to note that the amount of anticlastic bending produced in these tests is dependent upon the boundary conditions of the panels as well as upon the dimensions of the panels and, therefore, the resulting discrepancies are not uniquely characteristic of sandwich panels.

The results for panel D, tested under axial load only, are plotted in figures 14 and 18. Theoretically, the strain in the cover sheets should be compressive and uniform, and equal to σ_x/E_f in the elastic range. Examination of the results in figure 14 shows that the average experimental strain agrees with this value within 2 percent until near critical load. If there is no eccentricity present, the deflection of the panel should be zero to critical load and then increase to infinity at a very slight increase in load. Agreement between theory and experiment is good, although a slight eccentricity was probably present since the deflections, though small, are present at low loads. This is also borne out by the presence of small bending strains.

The deflections and strains of a panel under lateral pressure only were obtained by extrapolating the curves for combined load to zero axial load. The values so obtained are plotted in figures 22 and 23 as are the experimental results. For this loading, the theoretical results again are conservative and the nonagreement is attributed to anticlastic bending.

The flexural rigidity per inch of width of each group of panels having the same dimensions was computed from

$$(EI)_b = \left(E_f t^3/6\right) + \left[t(b + t)^2 E_f/2\right]$$

The flexural rigidity of the panel was computed by multiplying this value by the panel width in inches. The results are given in column (3) of table 4. Comparison with the experimentally determined values shows that the calculated values are low by about 3 percent in most cases.

There are, generally, three possible modes of failure for sandwich panels under combined axial and lateral loading; the one which occurs will be that requiring the lowest load. These types of failure and the loading conditions under which they may be expected are:

(a) Column - axial load high, lateral load zero or comparatively small

(b) Shear failure of core - lateral load high, axial load zero or comparatively small

(c) Local instability of compressed sheet - moderate lateral and axial loads causing strains in sheet to reach yield point

For the panels tested under combined load and under axial load alone, the column, or critical, loads were computed from average dimensions of the panels in a group by use of equation (20) and are given in column (7) of table 4. The axial load which, combined with the test lateral pressure, would cause local instability of the compressed sheet was taken as the load corresponding to the yield-point strain ϵ_{cy} of the sheet material (see table 2) read from the theoretical curves of figures 14 to 17. These values are given in column (8) of table 4. The axial load which, combined with the test lateral pressure, would cause shear failure can be approximately computed by assuming the deflection curve of the panels to be a half sine wave. If this is done, the maximum shearing stress is found to occur at the ends of the panel and to be given by

$$\tau_c = \left(\frac{qLw}{2} + \frac{P\pi d}{L}\right)\frac{t(b + t)}{2I} \tag{22}$$

where

τ_c maximum shear stress in core, psi

P axial load, $2\sigma t$, lb

d theoretical center deflection at load P, found from figures 18 to 21, in.

I computed moment of inertia of panel, $in.^4$

This relation is approximate insofar as the term $P\pi d/L$ is concerned, but since figures 18 to 21 show that the theoretical deflections are greater than the experimental ones, the stresses computed from this relation may be safely considered to be higher than the actual ones. If this stress is less than $\tau_{c,ult}$, the possibility of failure due to shearing of the core is eliminated. The stresses computed from this relation at the lesser of the loads in columns (7) and (8) of table 4 are given in column (9) of table 4. Except for panel H, these stresses

are all less than $\tau_{c,ult}$, which, averaging the first part of table 3, is about 290 psi. The predicted failure load for the other panels is the lesser of the two loads in columns (7) and (8) of table 4. No failure load was predicted for panel E which failed in an unusual manner because of imperfect fabrication.

An examination of table 4 shows that panel D, under axial load, failed as a column and that the panels tested under combined load failed by local instability of the compressed sheet. The percentage difference between the experimental and the predicted maximum loads is given in column (10), table 4. This difference varies from 4.3 percent to -8.7 percent.

For panel H tested under lateral load alone, failure due to column action is impossible. The lateral pressure required to produce failure due to yielding of the sheet, read from figure 22 as that value of lateral pressure corresponding to the yield-point strain, is 12.1 psi. The lateral pressure required to produce shear failure in the core was computed from the relation

$$q = \frac{4I\tau_{c,ult}}{L^{*}wt(b + t)} \tag{23}$$

where L^{*} is the loaded length of the panel, $L - 1$ in inches, and was found to be 9.36 psi. The actual maximum lateral pressure was 9.54 psi, which is only 1.9 percent greater than this.

DISCUSSION

The maximum load and the bending rigidity of the sandwich panels as obtained by test agreed well with theoretical values. For the panels tested under combined lateral and axial loads and under lateral load alone, the theory as extended in this report for columns under combined loading predicted strains and deflections larger than those obtained in the tests.

No anticlastic bending was considered in the basic assumption made in the analysis, namely, that the sandwich plates with simply supported loaded edges and free unloaded edges would react to combined loadings of lateral pressure and axial load in the same way and to the same extent as columns under those loadings. In the case of axial load alone, where the core is not subjected to large shearing strains and the panel to large bending strains, this assumption was warranted on the basis of the test made of the panel under axial load. This does not appear to be

entirely the case, however, for the panels under combined loading. Had the panels acted like columns, there would have been a uniform strain across the width of the panel. Actually, the strains at the center differed considerably from those at the edges (see fig. 13). The deflections showed a similar tendency, with the deflections at the center smaller than those nearer the free edges. These strain and deflection distributions indicate anticlastic bending.

It was assumed in the theoretical analysis that the column was initially compressed under axial load and the displacements were all taken from that condition. In the test, the panel was loaded axially, then increments of lateral pressure and axial load were put on until the test pressure was reached, and finally only the axial load was increased until failure. The sequence of loading may have an effect on the strains and deflections where nonlinearity is present, but, in similar loading on a sheet-stringer panel (ref. 3), the sequence of loading was found to have no effect. No effect is therefore believed to have been present in the tests reported herein.

The assumption that the core carries a negligible amount of the axial load seems justified from the results of the test of panel D under axial load because the measured and computed average strains (fig. 14) agree within 2 percent until near the failing load.

In the calculations, the average value of the shear modulus was used as determined from two tests of samples of 1/2-inch-thick sandwich with 0.032-inch-thick facings (specimens 4 and 6, table 3). This average value, 83,800 psi, agreed fairly well with the value 77,590 psi obtained in another investigation at the Forest Products Laboratory[1]. Although the modulus should be independent of thickness of core, it is not known whether this is actually the case. There is some scatter in the value of G, but it is not likely that this would account for the observed differences between theoretical and experimental results.

The nominal thicknesses of the cover sheets were used in all calculations as it was too difficult to obtain the actual values accurately from the assembled panels. Since the weights of similar panels are in close agreement, it is believed that the actual values differed little from the nominal values.

Of the above possible causes of discrepancy between theoretical and experimental results, anticlastic bending is considered the primary cause.

---

[1]Letter from Forest Products Laboratory, November 24, 1950.

CONCLUSIONS

On the basis of the analysis made, it can be concluded that, for sandwich plates with the loaded edges simply supported and the unloaded edges free:

1. The theory for buckling of simply supported sandwich columns under axial load is applicable to sandwich plates under axial load.

2. The failing loads of sandwich panels under combined load and under lateral pressure alone can be predicted with satisfactory accuracy.

3. The formulas for the axial strain and lateral deflections of sandwich plates under compressive axial load and lateral load as derived from the theory for columns are conservative in most cases.

National Bureau of Standards,
Washington, D. C., October 24, 1952.

APPENDIX A

EFFECT OF OVERLAPPING BAG IN COMBINED-LOADING TESTS

It was observed that the cloth air bag overlapped the unloaded edges of the panels in the form of a semicylinder of about 1/2-inch radius (see fig. 27). The force F thus exerted on one edge of the panel is seen to be equal to the sum of the vertical components of the pressure q' acting on quadrant AB of the cylinder. By integration it is found that $F = rq'L$ or that the total added force on the panel is $2F = 2rq'L$, where L is the length of the panel. With $r = 1/2$ inch and $w = 16.8$ inches, the average pressure q on the panel becomes

$$q = \frac{q'Lw + 2rq'L}{Lw}$$

$$= \frac{q'(w + 2r)}{w}$$

$$= 1.0595q'$$

The equivalent pressure is therefore about 6 percent higher than the bag pressure.

APPENDIX B

EFFECT OF IMPERFECT BEARING OF AIR BAG IN LATERAL-LOAD TEST

At the start of the lateral-load test, the rubber air bag bore upon the entire panel area. At an indicated pressure of 14 psi, it was estimated that, because of the approximately elliptical cross section which the bag had assumed, it no longer bore on 4 inches of panel width, 2 inches on each side. Assuming that the loaded area decreased linearly with indicated pressure,

$$w_{act} = w - \frac{4}{14}q_{ind}$$

$$= w - 0.286q_{ind}$$

where

w_{act} width of panel loaded, in.

w total panel width, in.

q_{ind} indicated manometer pressure, psi

The average pressure on the panel was taken as the pressure in the bag multiplied by the ratio w_{act}/w.

APPENDIX C

SYMBOLS

The following symbols are used in the sections "Theoretical Analysis" and "Comparison of Experimental Results With Theory." Symbols in other parts of the paper are defined where they appear.

b	core thickness, in.
d	panel deflection at midlength, in.
E_f	Young's modulus of face material, 10.5×10^6 psi
$(EI)_b$	bending rigidity of sandwich panel, $(EI)_1 + 2(EI)_f$
$(EI)_f$	bending rigidity of one face alone, $E_f t^3/12$
$(EI)_1 = t(b + t)^2 E_f/2$	
G	shear modulus of core, 83,800 psi
I	computed moment of inertia of panel, in.^{4}
L	length of column, in.
P	axial load, $2\sigma t$, lb
P_{cr}	critical buckling load, lb
P_{max}	maximum experimental axial load, lb
q	lateral load, psi
t	thickness of one facing sheet, in.
U	strain energy
u	change in displacement in x-direction due to applying lateral pressure (in positive x-direction on upper sheet, in negative x-direction in lower sheet, fig. 26), in.
V	potential of lateral and axial loads

v	lateral displacement of midthickness of core, in.
w	panel width, in.
x	distance from center along longitudinal center line, in.
γ_1, γ_2	angle of shear due to u and v, respectively
ϵ_{cy}	compressive yield strain of sheet material
ϵ_x	axial strain at midthickness of face
σt	compressive load acting on one face, lb
σ_x	axial stress at midthickness of faces, psi
τ_c	maximum shear stress in core, psi

Primed letters are derivatives with respect to x; that is, $u' = du/dx$.

REFERENCES

1. Hoff, N. J., and Mautner, S. E.: Bending and Buckling of Sandwich Beams. Jour. Aero. Sci., vol. 15, no. 12, Dec. 1948, pp. 707-720.

2. Anon.: Methods for Conducting Mechanical Tests of Sandwich Construction at Normal Temperatures. Rep. No. 1556, Forest Products Lab., U. S. Dept. Agric., revised Oct. 1948.

3. McPherson, A. E., Levy, Samuel, and Zibritosky, George: Effect of Normal Pressure on Strength of Axially Loaded Sheet-Stringer Panels. NACA TN 1041, 1946.

TABLE 1.- DESCRIPTION OF PANELS

Group	Panel	Length, in.	Width, in.	Over-all thickness, in.	Nominal sheet thickness, in.	Weight, lb
I	A	29.91	16.81	0.4903	0.025	3.62
	B	29.90	16.82	.4939	.025	3.68
	C	29.84	16.81	.4916	.025	3.70
	D	29.85	16.81	.4952	.025	3.74
II	E	29.89	16.85	.5009	.032	4.32
	F	29.90	16.83	.4983	.032	4.32
	G	29.90	16.88	.5001	.032	4.30
	H	29.91	16.88	.5025	.032	4.31
III	I	29.90	16.78	.7417	.025	4.15
	J	29.90	16.78	.7388	.025	4.13
IV	K	29.94	16.85	.7441	.032	4.93
	L	29.94	16.85	.7433	.032	4.89

TABLE 2.- TENSILE AND COMPRESSIVE PROPERTIES OF SHEET

[See also fig. 2]

Specimen	Nominal thickness of sheet, in.	Young's modulus, psi	Yield strength (offset, 0.2 percent), psi	Yield strain (offset, 0.2 percent)	Ultimate strength, psi
Tension					
T1	0.025	10.2×10^6	68,000	0.0086	74,000
T2	.025	10.4	68,000	.0086	78,000
Av.	.025	10.3	68,000	.0086	76,000
T3	.032	10.3	75,000	.0092	(a)
T4	.032	10.3	73,000	.0091	81,000
T5	.032	10.3	72,000	.0094	80,000
Av.	.032	10.3	73,000	.0092	80,000
Compression					
C5	0.025	10.5×10^6	64,000	0.0080	------
C6	.025	10.5	64,000	.0081	------
Av.	.025	10.5	64,000	.0080	------
C3	.032	10.5	67,000	.0084	------
C4	.032	10.2	68,000	.0087	------
Av.	.032	10.4	68,000	.0086	------

[a]Not measured.

TABLE 3.- SHEAR PROPERTIES OF CORE[a]

[See also fig. 3]

Specimen	Strength, psi	Modulus of rigidity, psi	Secant modulus at maximum stress, psi
Deformation parallel to core strip direction			
2	278	[b]204,000	[b]16,500
4	---	81,000	------
6	301	86,000	25,400
Deformation perpendicular to core strip direction			
1	200	23,400	4,370
3	178	26,800	5,000
5	181	28,300	6,900

[a]From tests performed by the Forest Products Laboratory.

[b]Value should be disregarded.

TABLE 4.- COMPARISON OF EXPERIMENTAL AND CALCULATED VALUES

(1)	(2)	(3)	(4)	(5)	(6)	(7)	(8)	(9)	(10)
Panel	Flexural rigidity			Lateral pressure, psi	P_{max}, exp., lb	P_{cr}, calc. eq.(20), lb	P at $\epsilon_x = \epsilon_{cy}$, lb	τ_c,[a] calc. eq.(22), psi	Difference,[b] percent
	Exp., lb-in.^{2}	Calc., lb-in.^{2}	Difference, percent						
A	5.0×10^5	4.83×10^5	3.3	0.794	4,200	4,920	4,320	180	-2.8
B				1.58	3,750		3,830	200	-2.1
C				2.13	3,630		3,480	210	4.3
D				0	5,030		70,600	0	2.2
E	6.4	6.23	2.7	1.06	5,130	6,330	(c)	---	---
F				2.11	4,900		4,860	260	.8
G				2.66	4,520		4,620	280	-2.2
H				[d]9.54	0		0	300	---
I	11.7	11.27	2.8	1.71	8,800	11,400	9,530	190	-7.7
J				3.42	7,300		7,680	200	-4.9
K	14.5	14.35	.9	2.15	11,300	14,400	12,380	270	-8.7
L				4.28	9,310		10,110	270	-7.9

[a]At lesser of loads in columns (7) and (8).
[b]Between column (6) and lesser of columns (7) and (8).
[c]Panel improperly fabricated.
[d]Maximum.

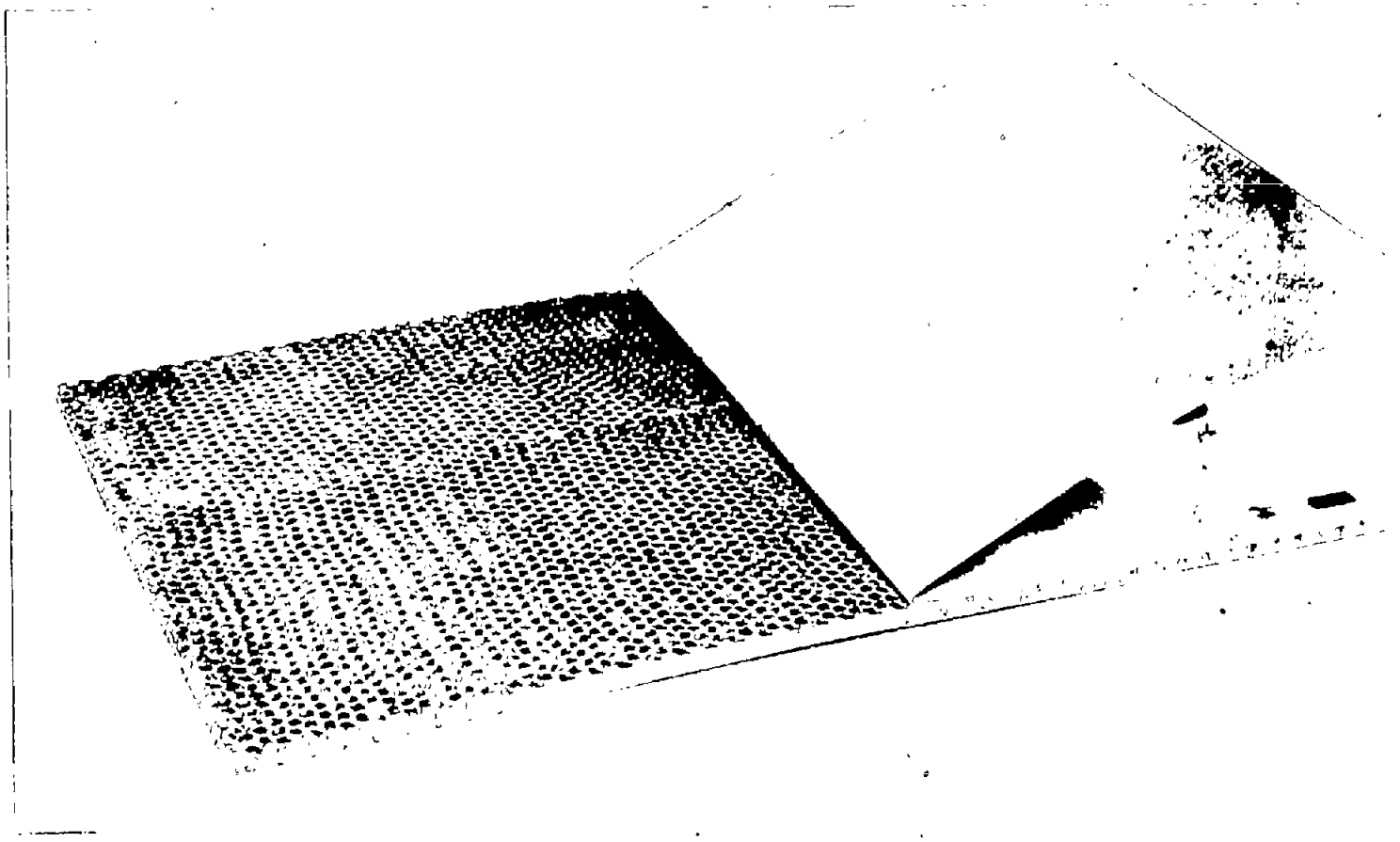

L-80270

Figure 1.- Aluminum honeycomb sandwich panel, with one sheet partially removed to show core.

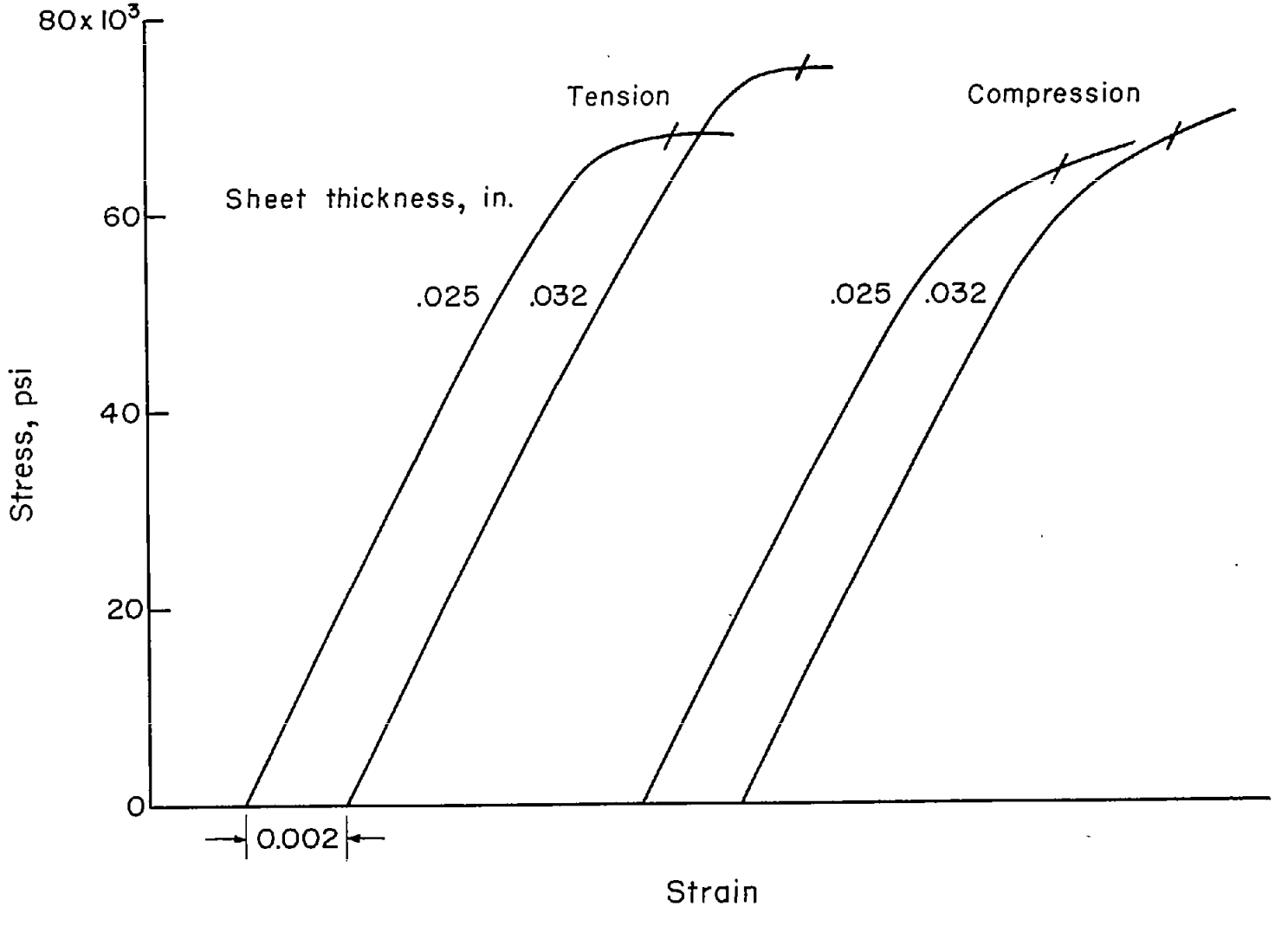

Figure 2.- Representative tensile and compressive stress-strain curves of sheet material in direction of rolling.

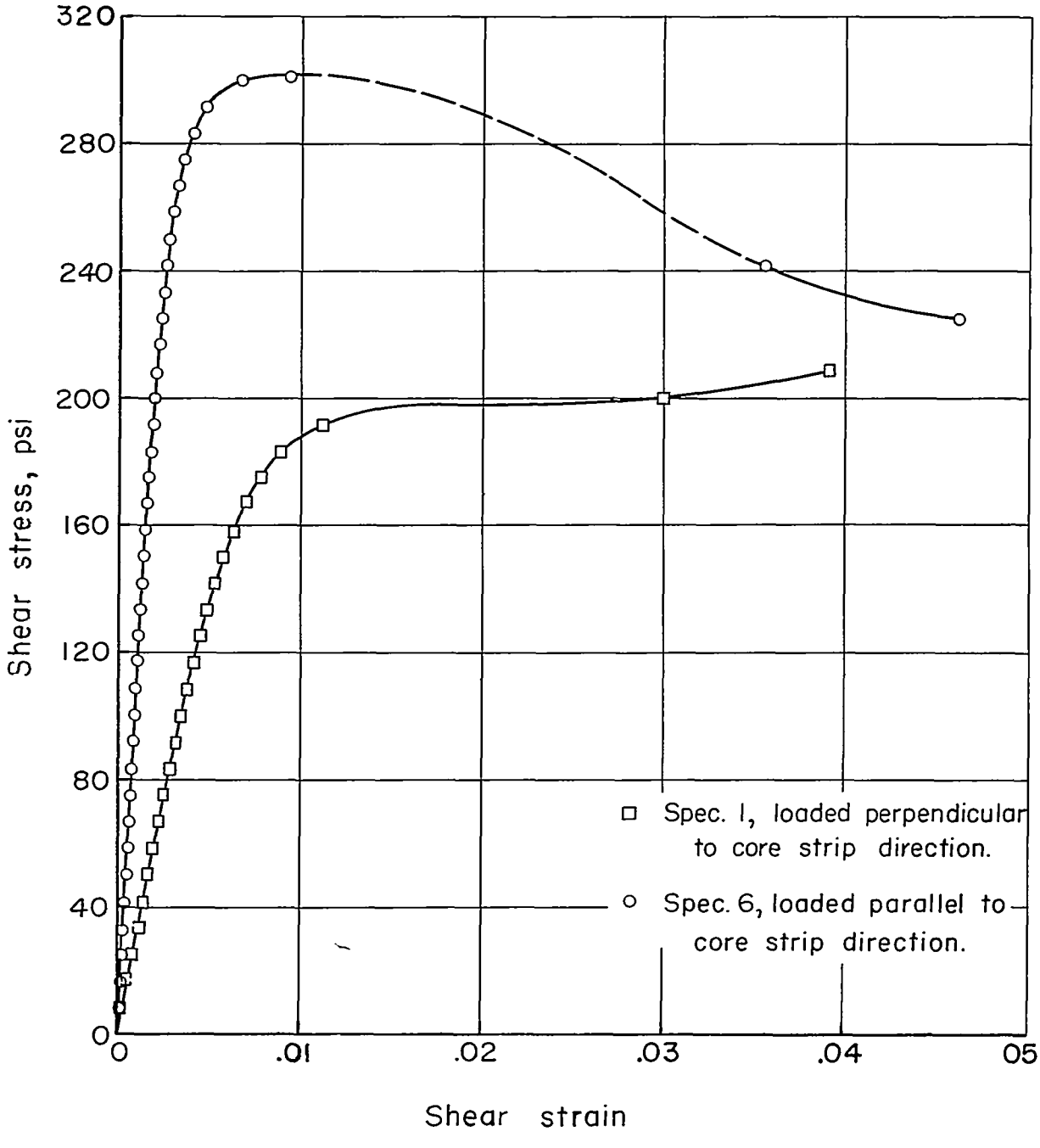

Figure 3.- Shear stress-strain curves for core.

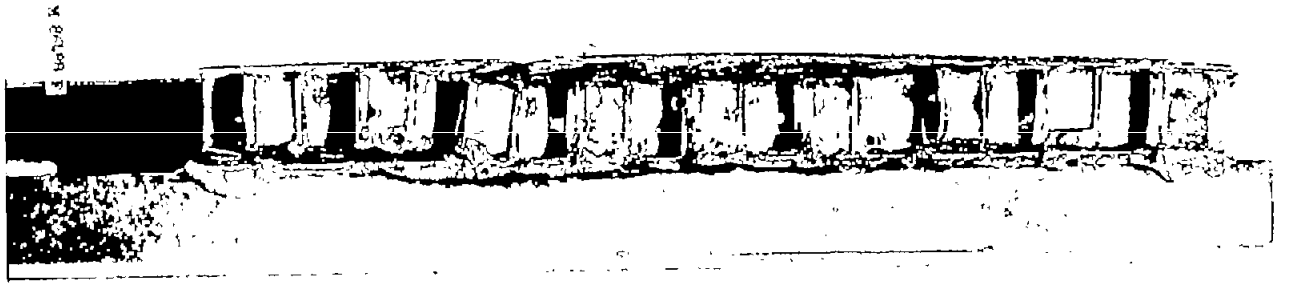

(a) Loaded parallel to core strip direction.

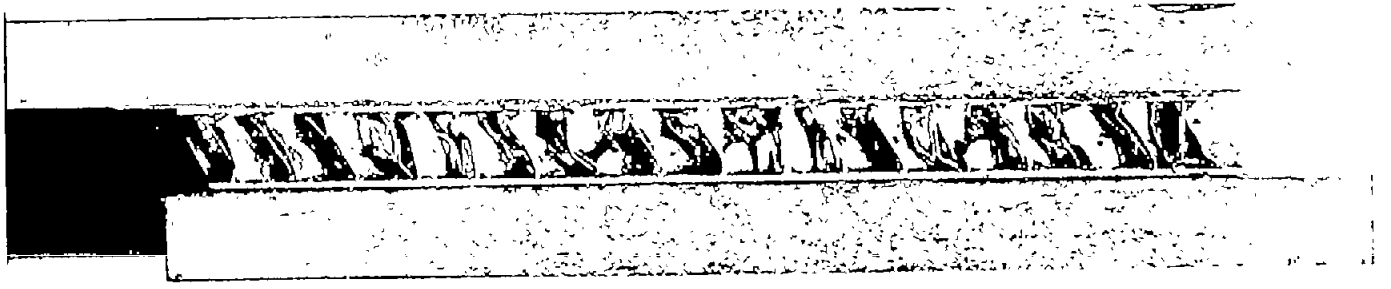

L-80271

(b) Loaded perpendicular to core strip direction.

Figure 4.- Failures of core in shear.

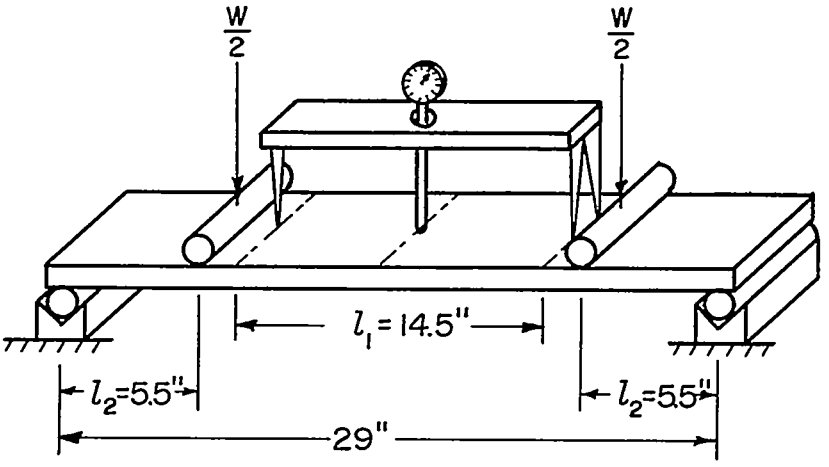

(a) Schematic drawing of test setup.

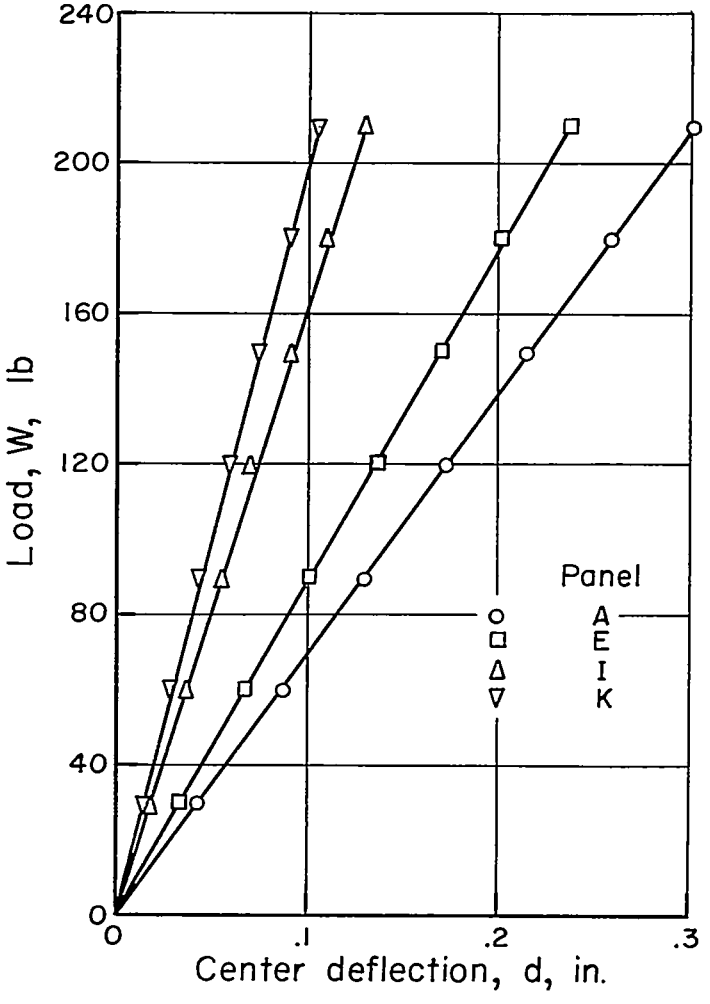

(b) Load-deflection curves.

Figure 5.- Flexural rigidity of sandwich material.

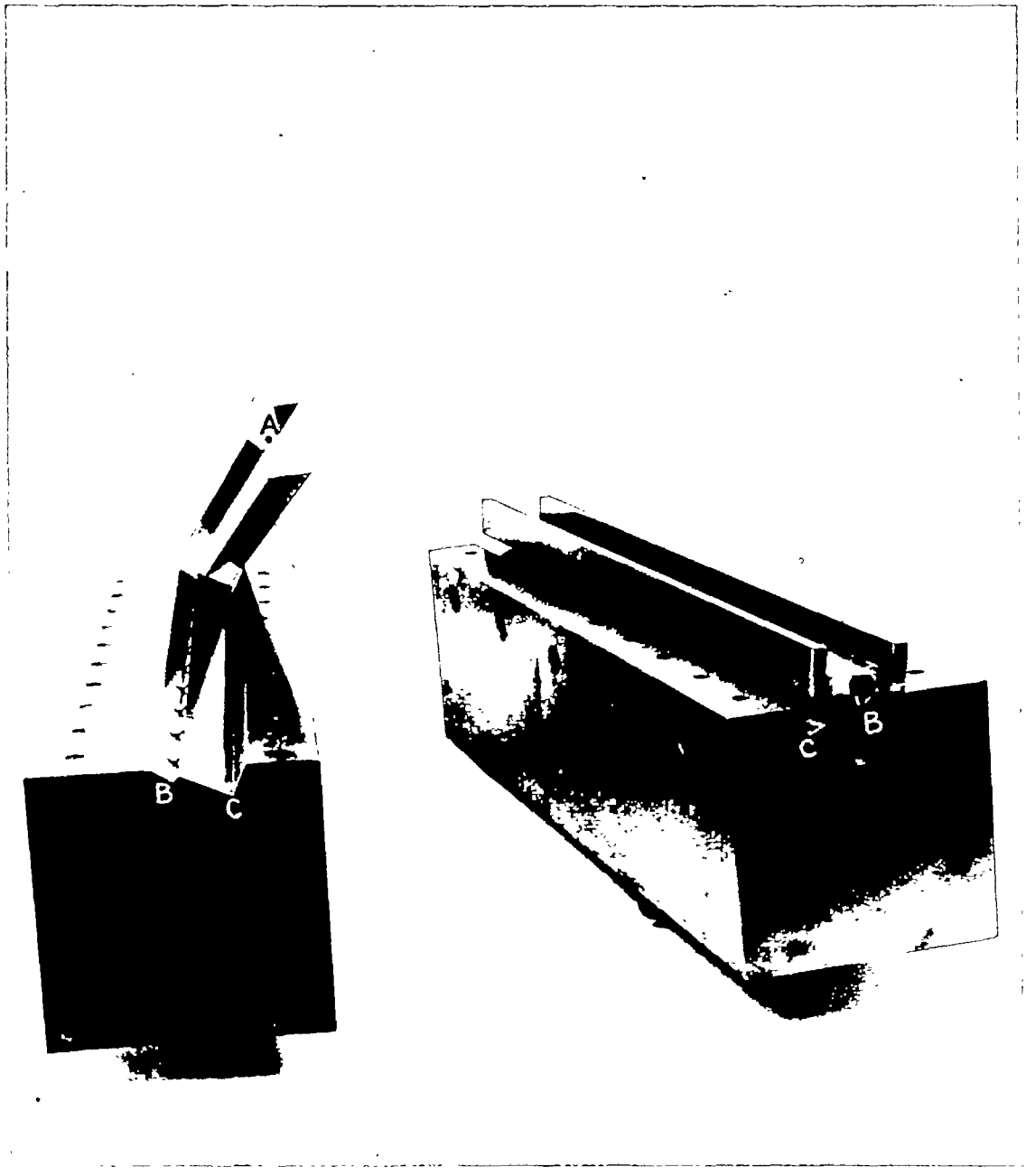

L-80272

(a) Knife edge and knife-edge seat. (b) Assembled position.

Figure 6.- Knife-edge fixtures and bearing blocks.

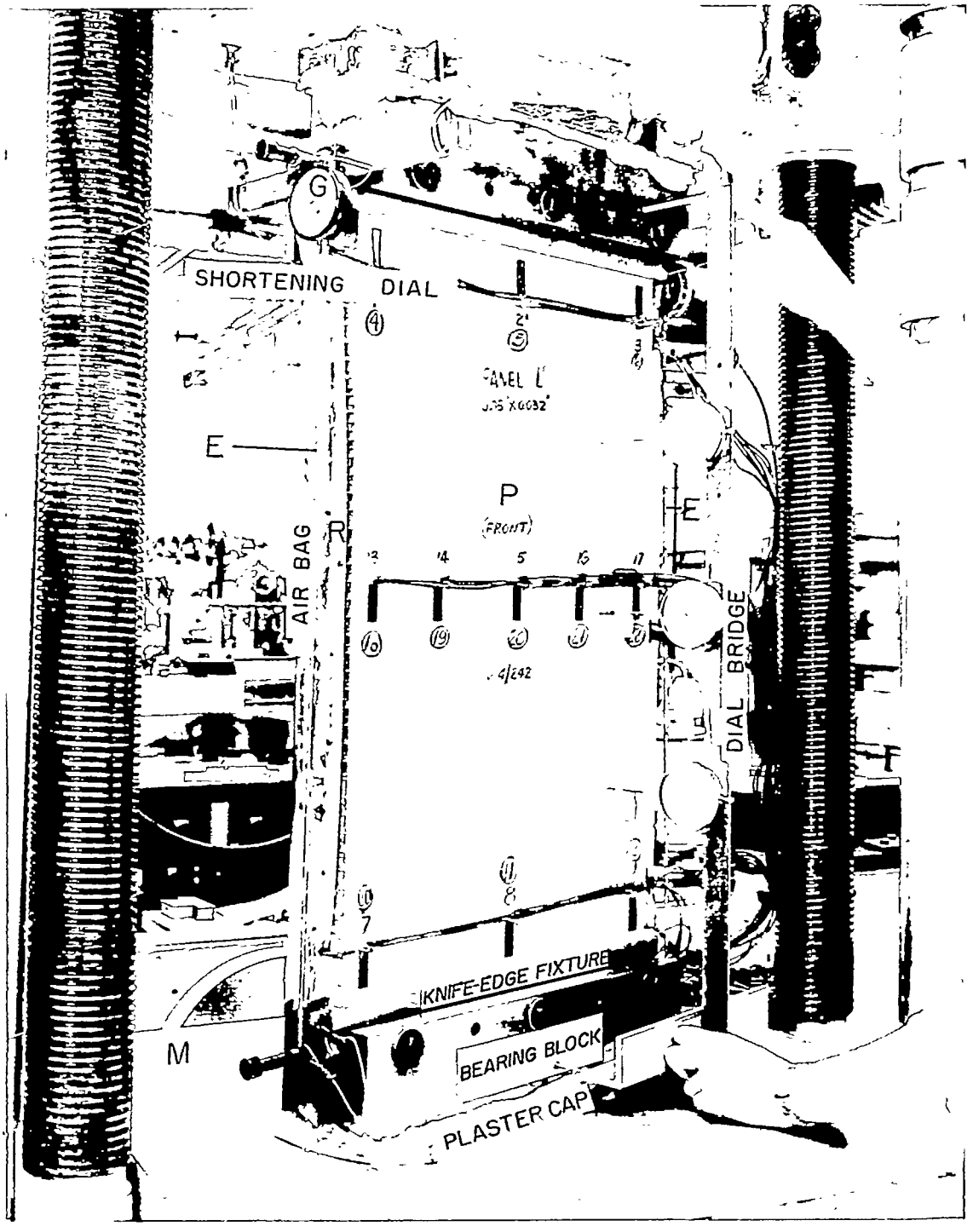

L-80273

Figure 7.- Combined-loading test setup, front view.

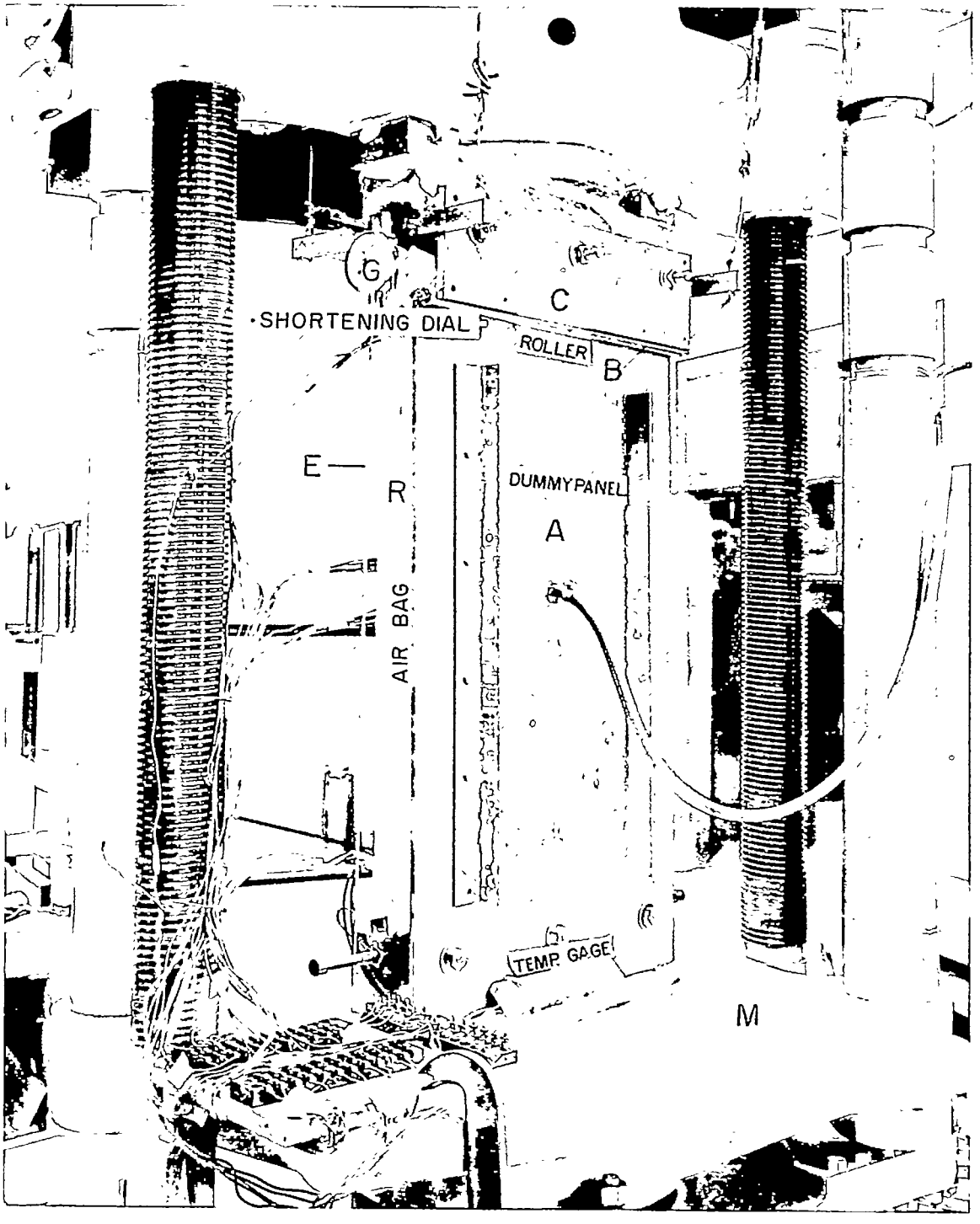

L-80274

Figure 8.- Combined-loading test setup, rear view.

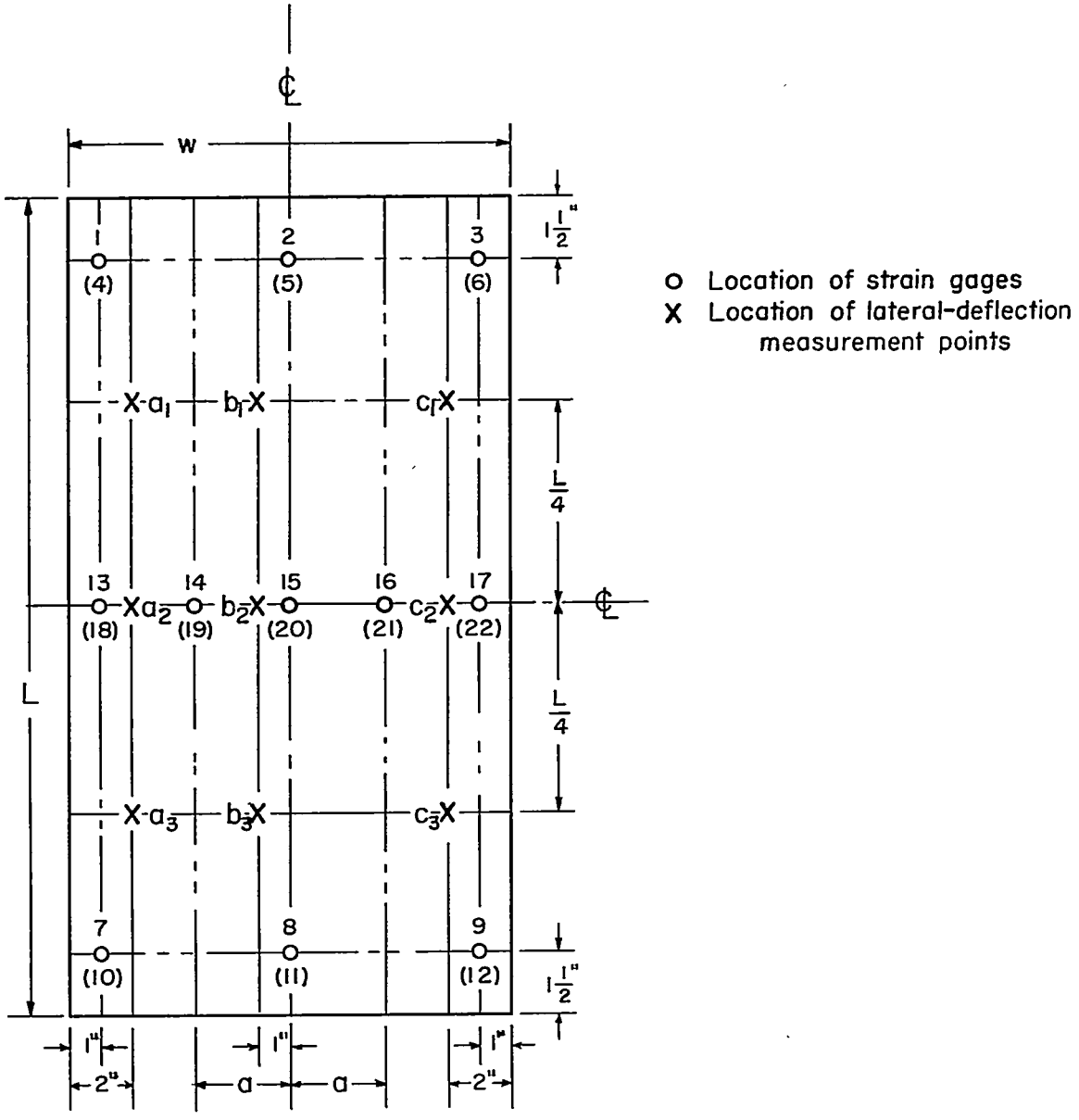

Figure 9.- Location of strain gages and lateral-deflection measurement points. Numbers in parentheses refer to strain gages on reverse face of panel. $a = \frac{1}{2}\left(\frac{w}{2} - 1\right)$ in inches.

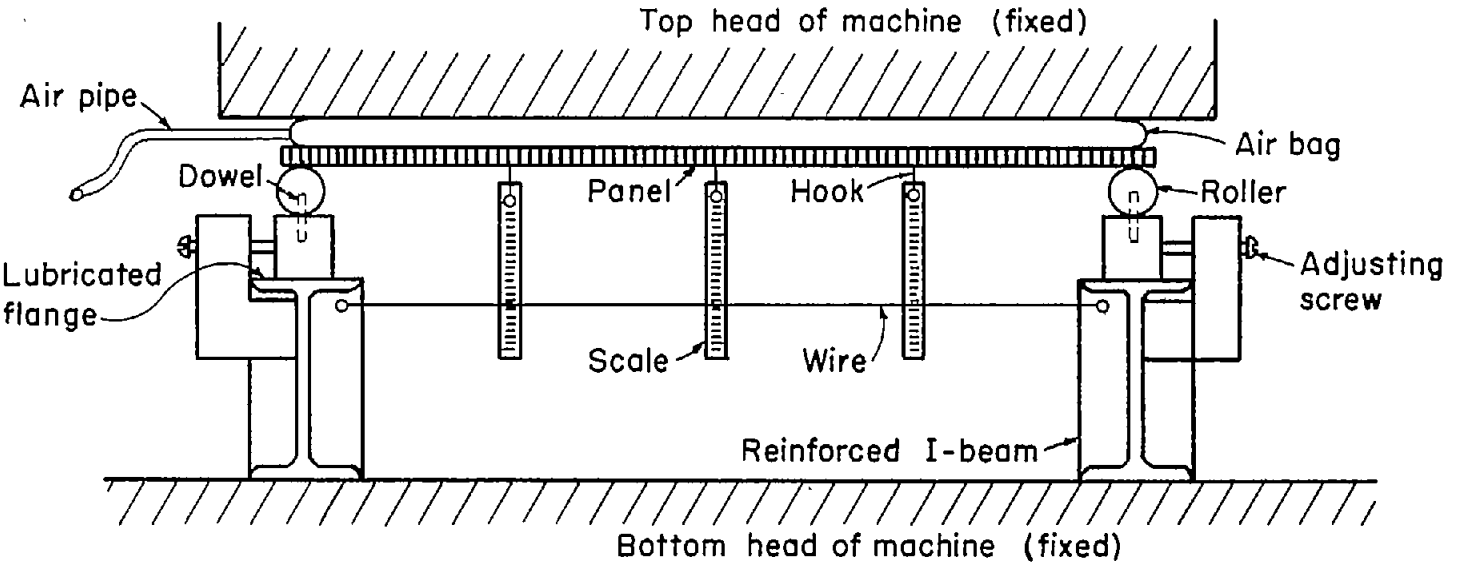

Figure 10.- Schematic drawing of setup for test of panel H under lateral pressure alone.

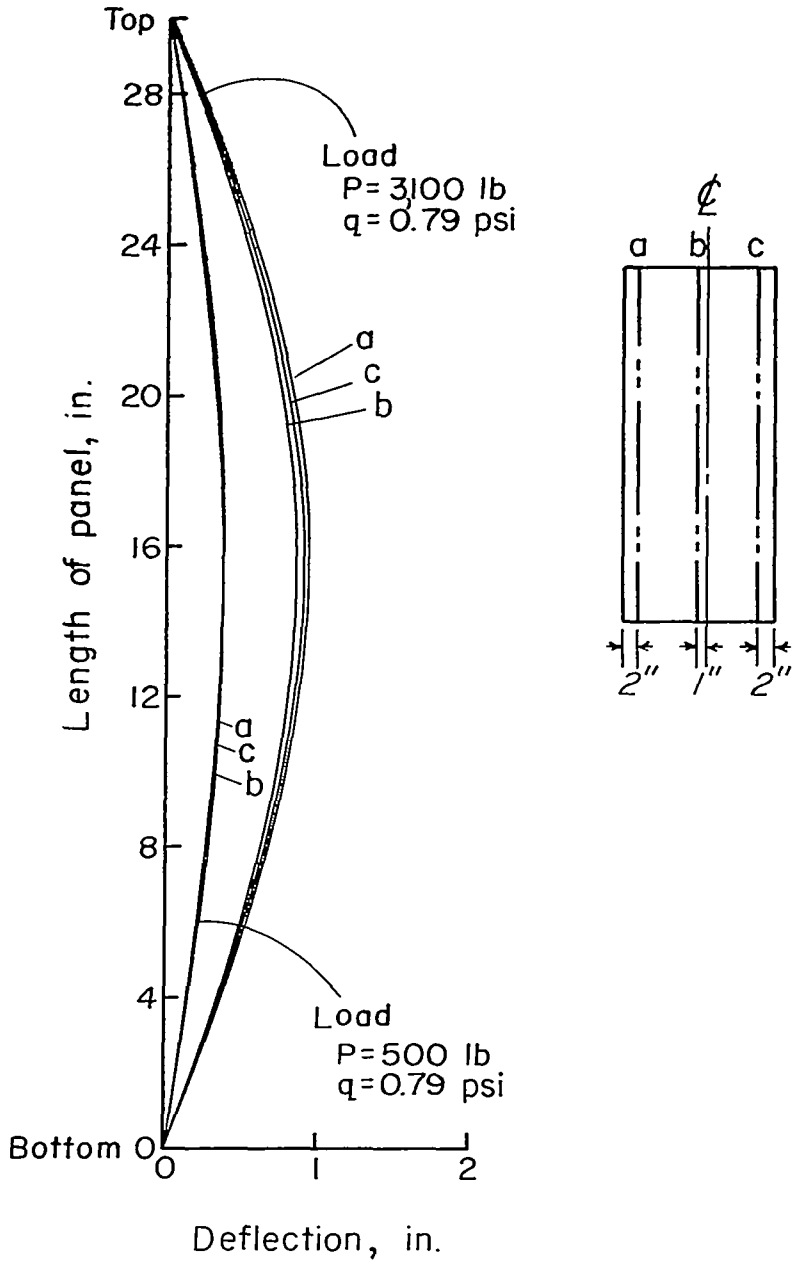

Figure 11.- Laterally deflected shape of panel A. (See also fig. 9.)

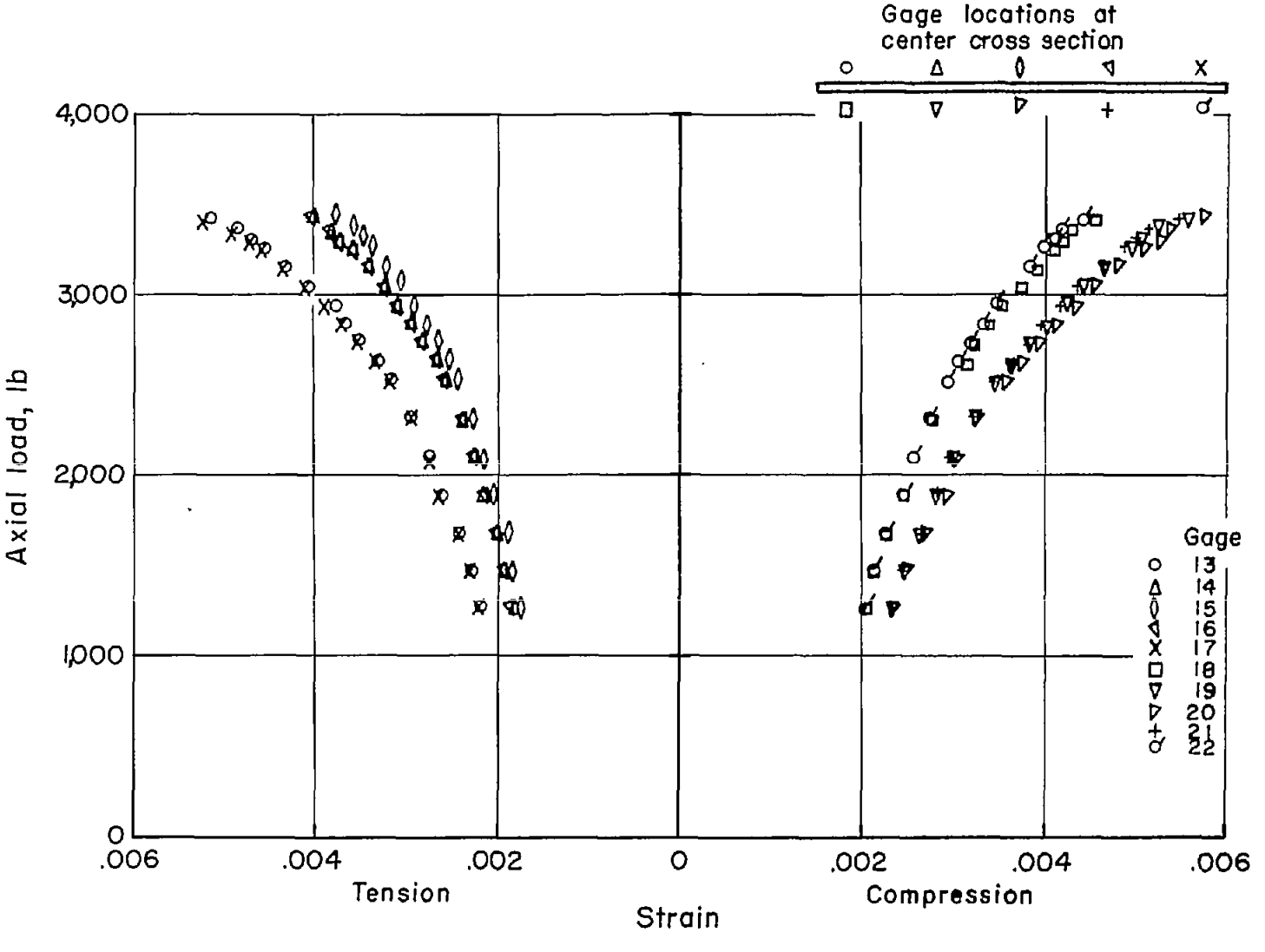

Figure 12.- Load-strain curves of 10 center strain gages of panel B. Axial load, 3,050 pounds; lateral pressure, 1.58 psi.

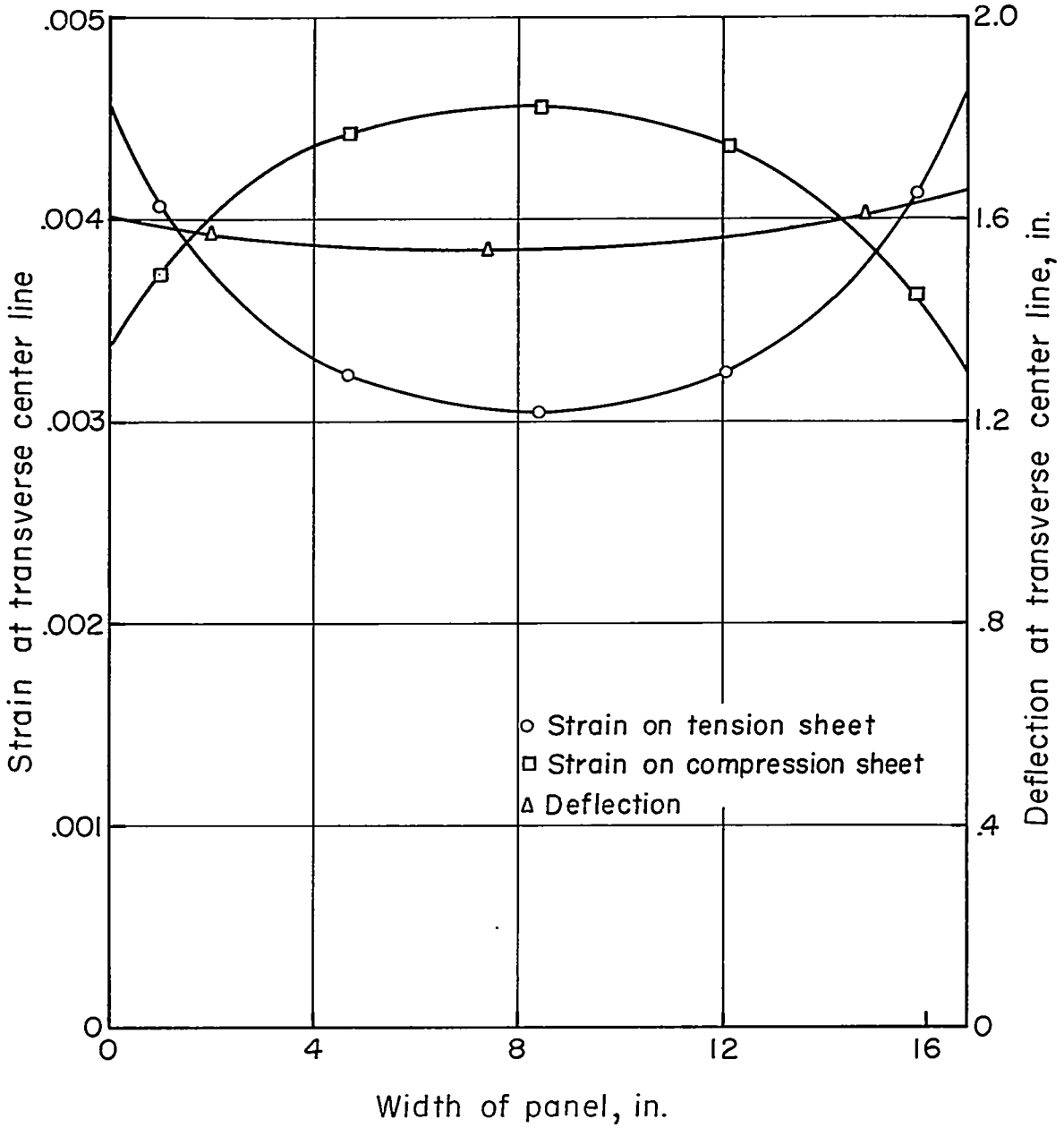

Figure 13.- Transverse strain and deflection distribution. Panel B; axial load, 3,050 pounds; lateral pressure, 1.58 psi.

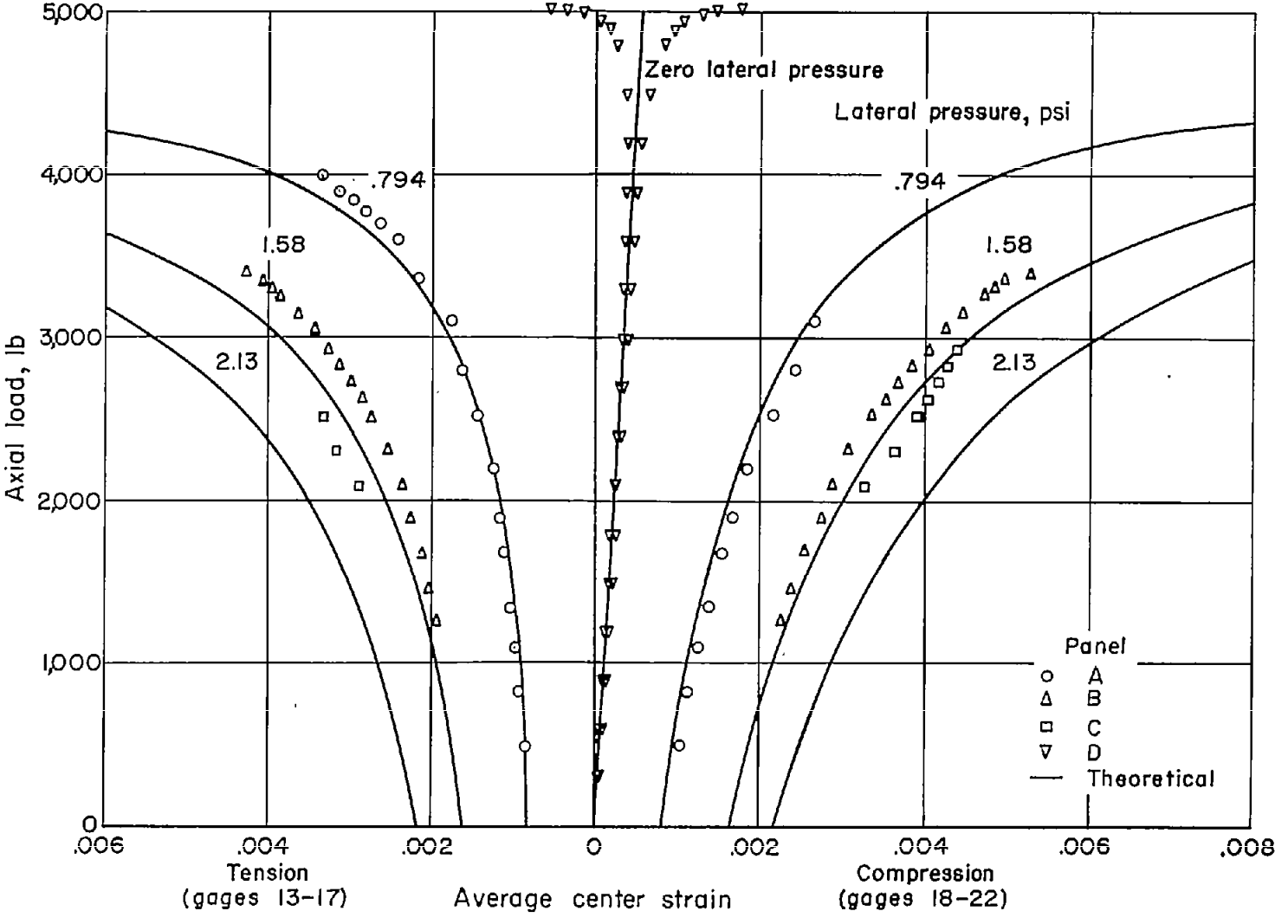

Figure 14.- Axial load against average center strain for panels 1/2 inch thick with faces of 0.025-inch aluminum-alloy sheet.

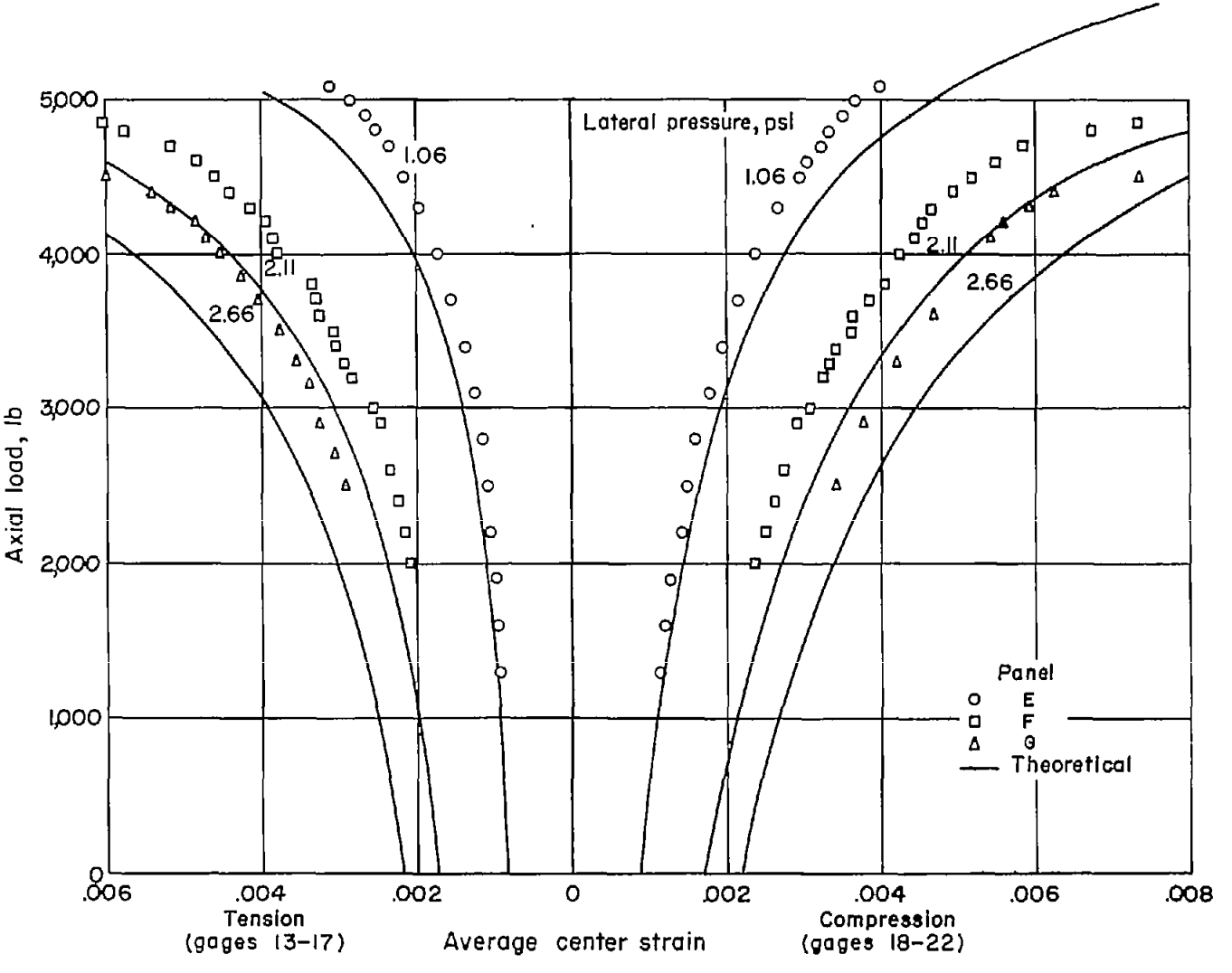

Figure 15.- Axial load against average center strain for panels 1/2 inch thick with faces of 0.032-inch aluminum-alloy sheet.

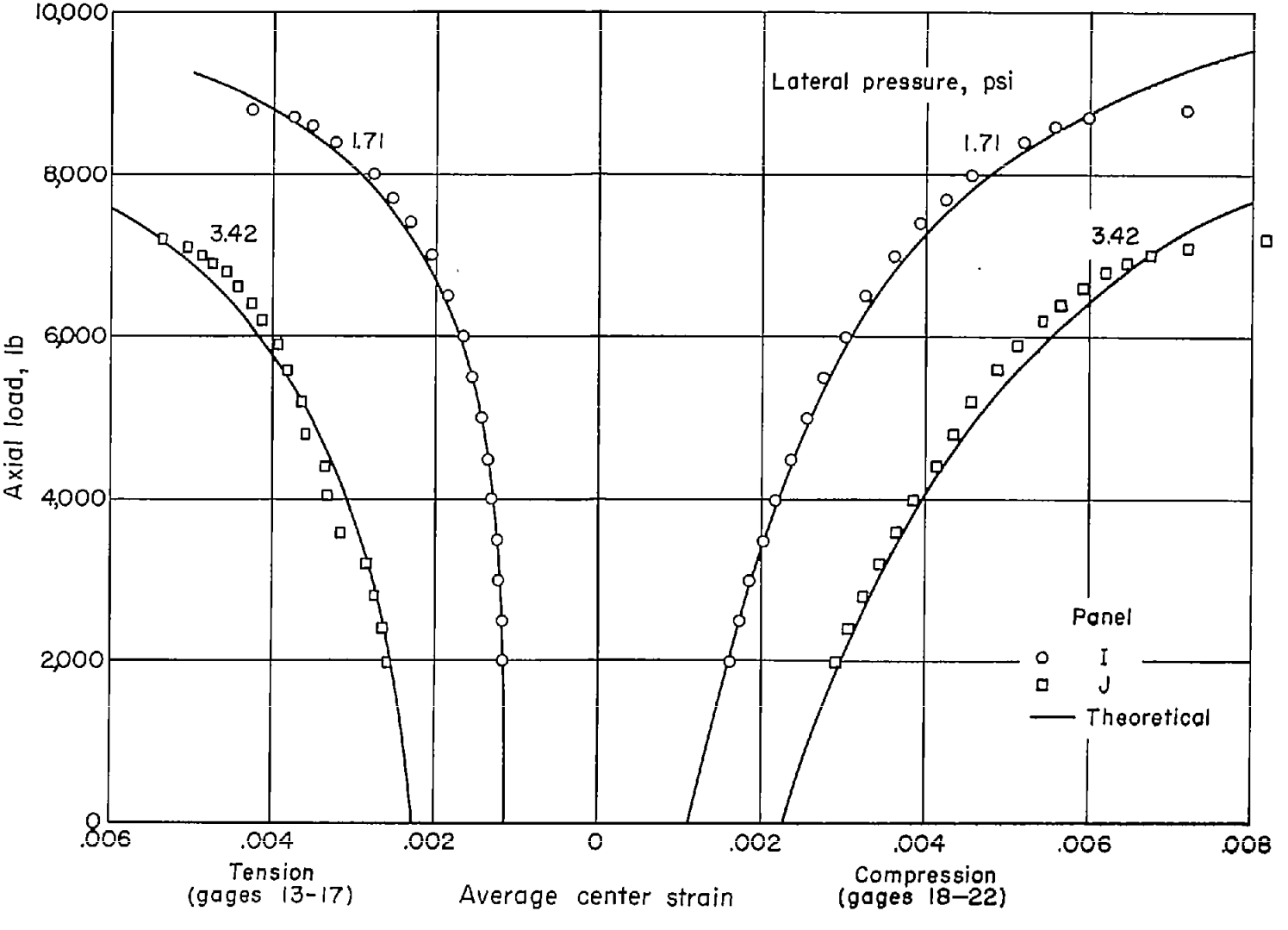

Figure 16.- Axial load against average center strain for panels 3/4 inch thick with faces of 0.025-inch aluminum-alloy sheet.

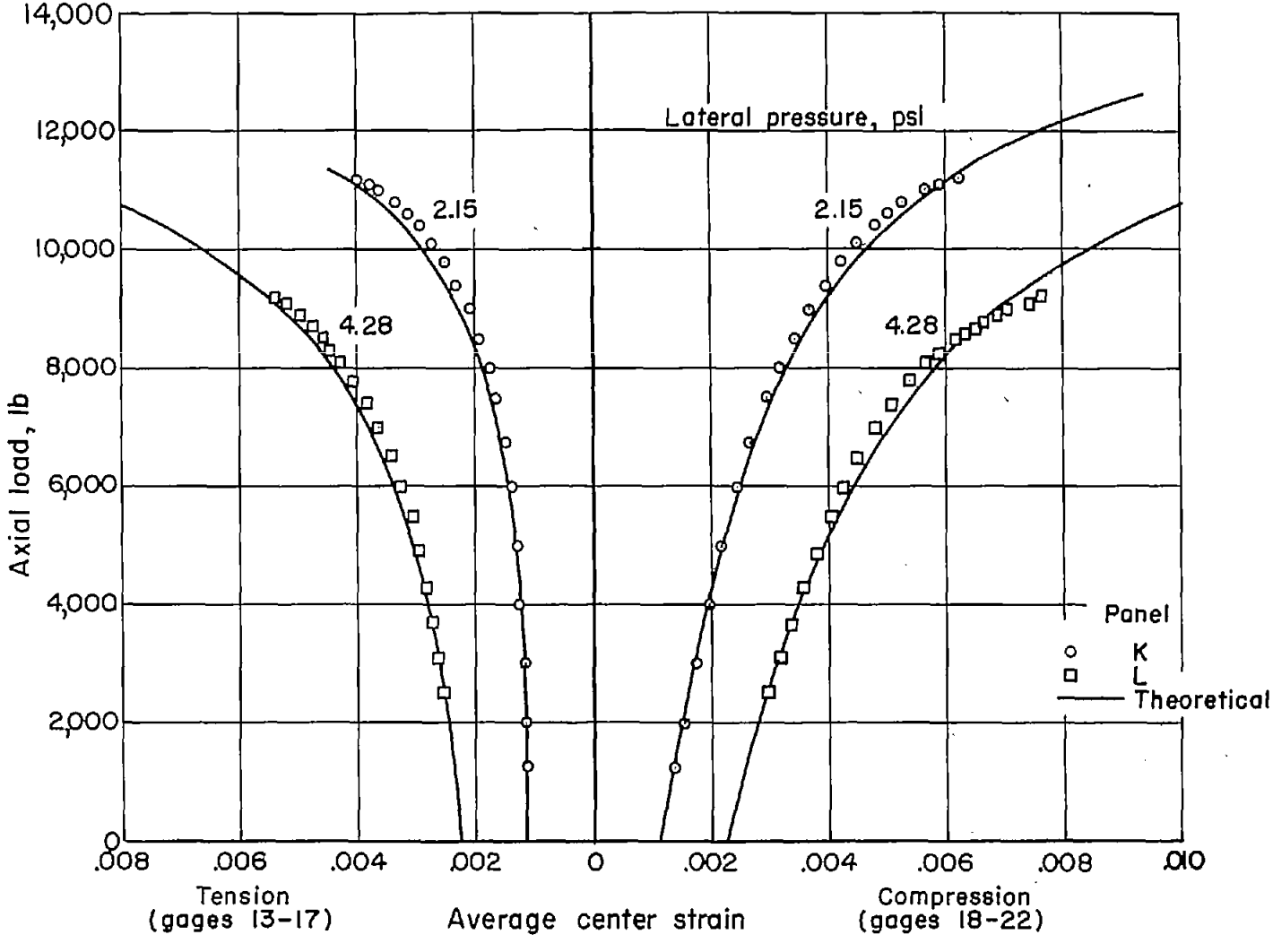

Figure 17.- Axial load against average center strain for panels 3/4 inch thick with faces of 0.032-inch aluminum-alloy sheet.

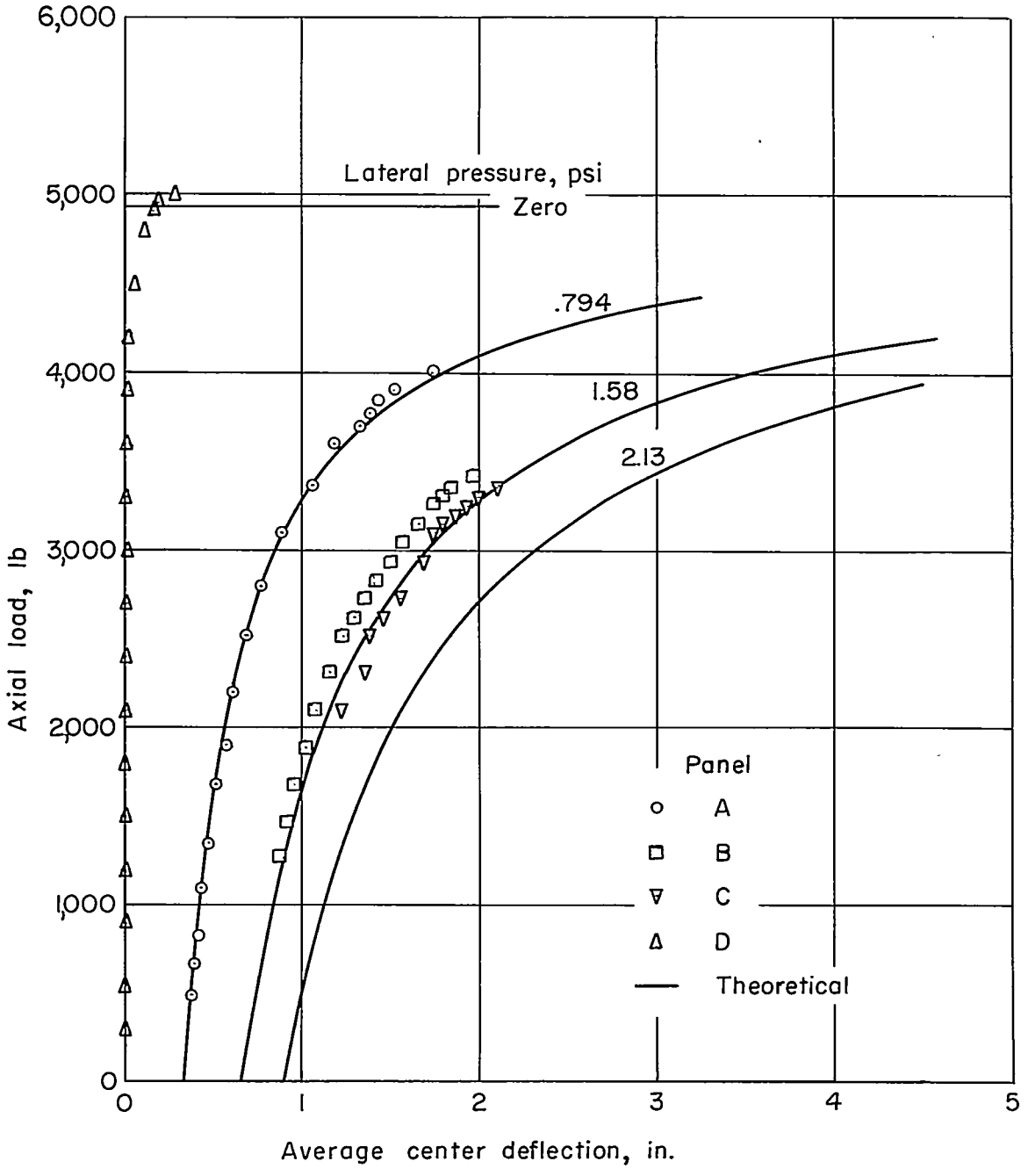

Figure 18.- Axial load against average center deflection for panels 1/2 inch thick with faces of 0.025-inch aluminum-alloy sheet.

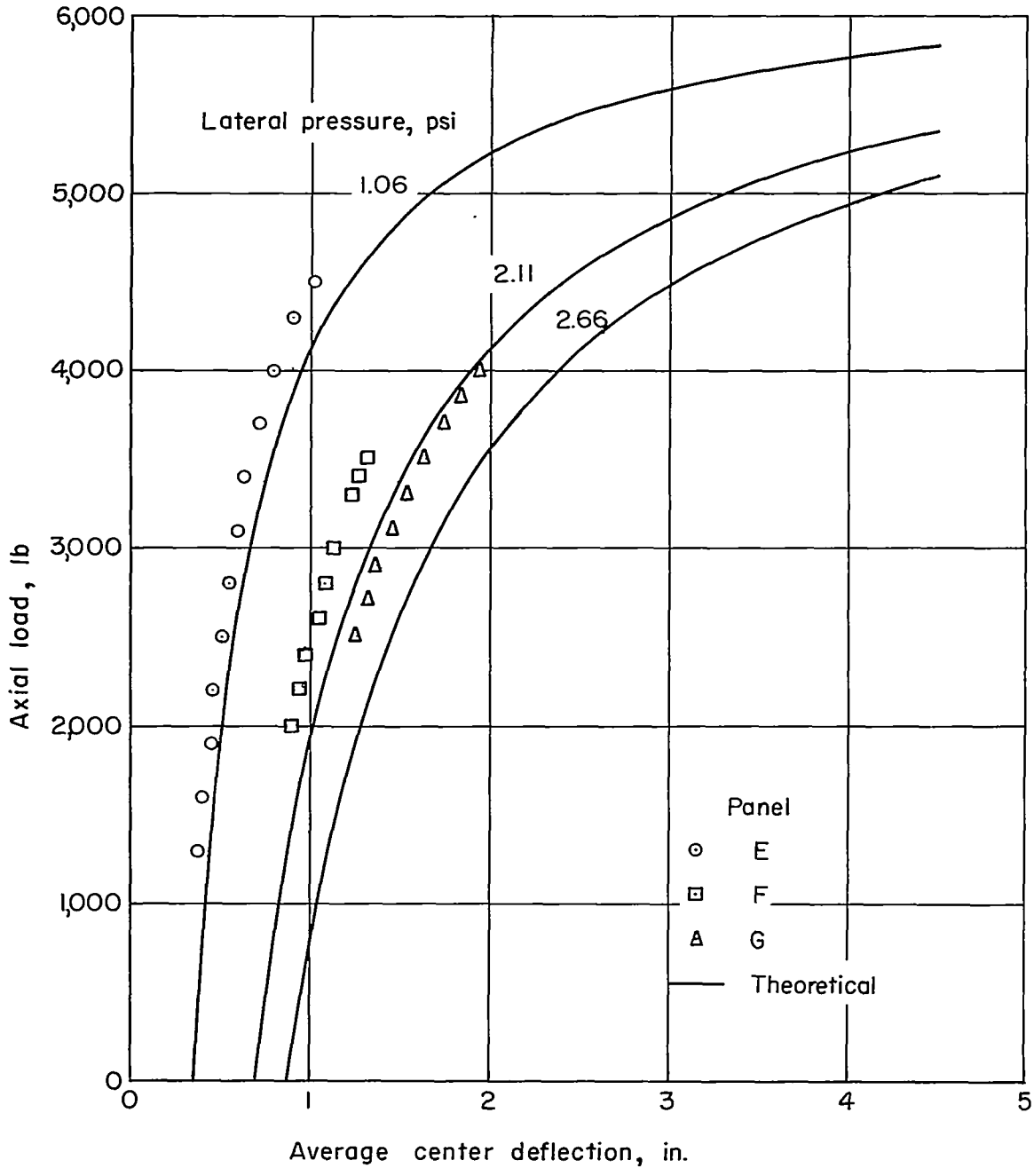

Figure 19.- Axial load against average center deflection for panels 1/2 inch thick with faces of 0.032-inch aluminum-alloy sheet.

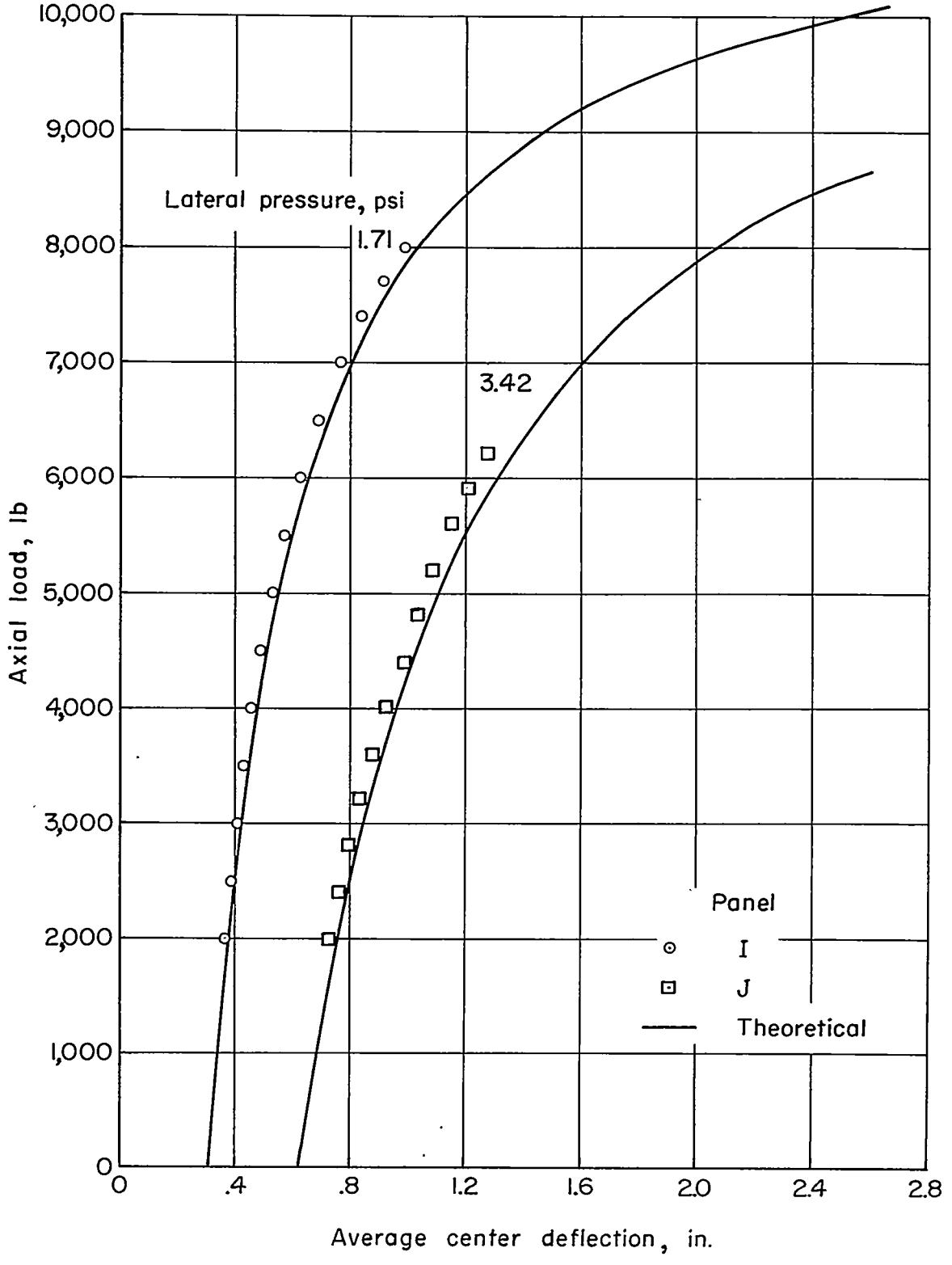

Figure 20.- Axial load against average center deflection for panels 3/4 inch thick with faces of 0.025-inch aluminum-alloy sheet.

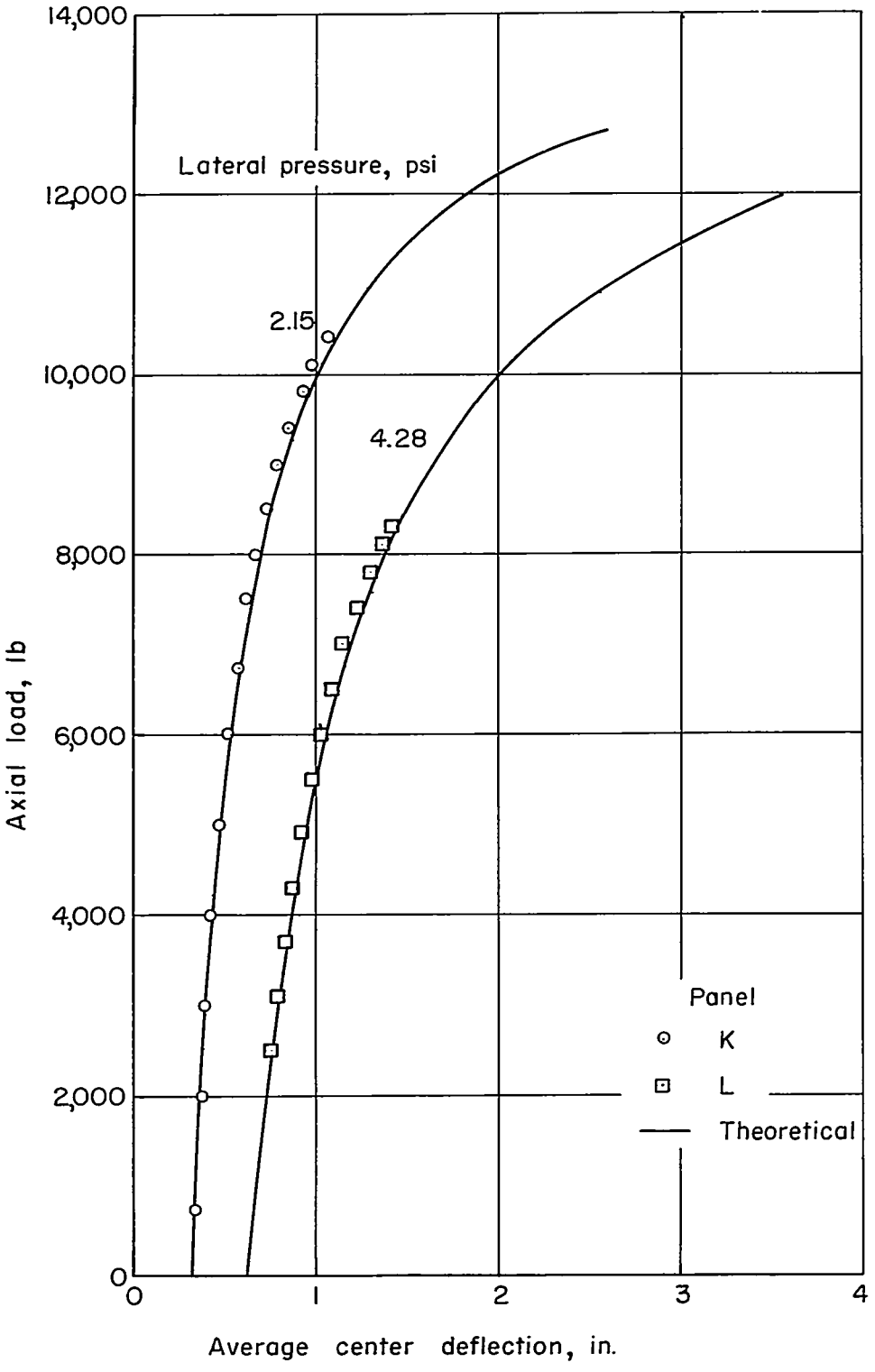

Figure 21.- Axial load against average center deflection for panels 3/4 inch thick with faces of 0.032-inch aluminum-alloy sheet.

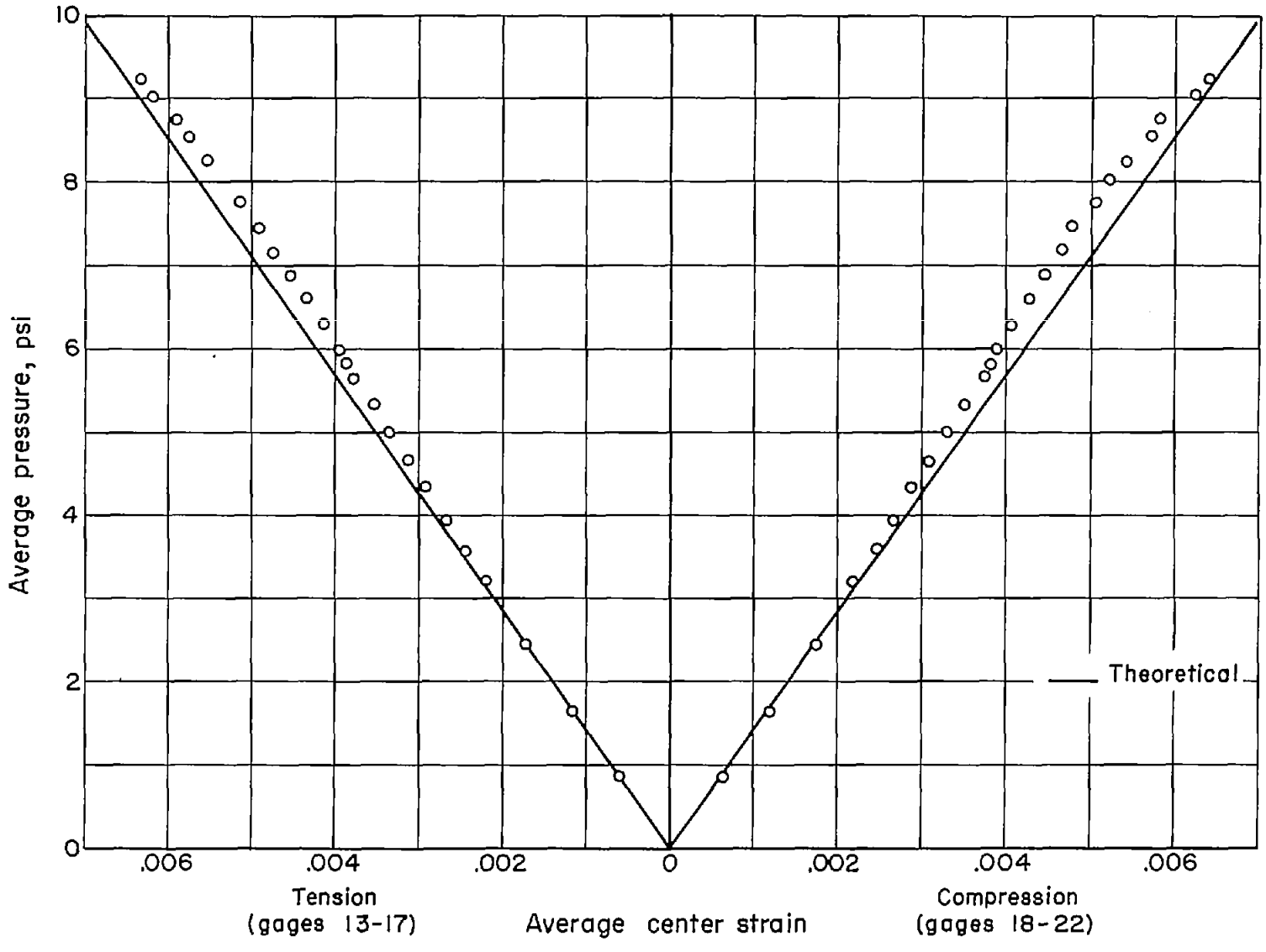

Figure 22.- Average lateral pressure against average center strain for lateral-load test of panel H 1/2 inch thick with faces of 0.032-inch aluminum-alloy sheet.

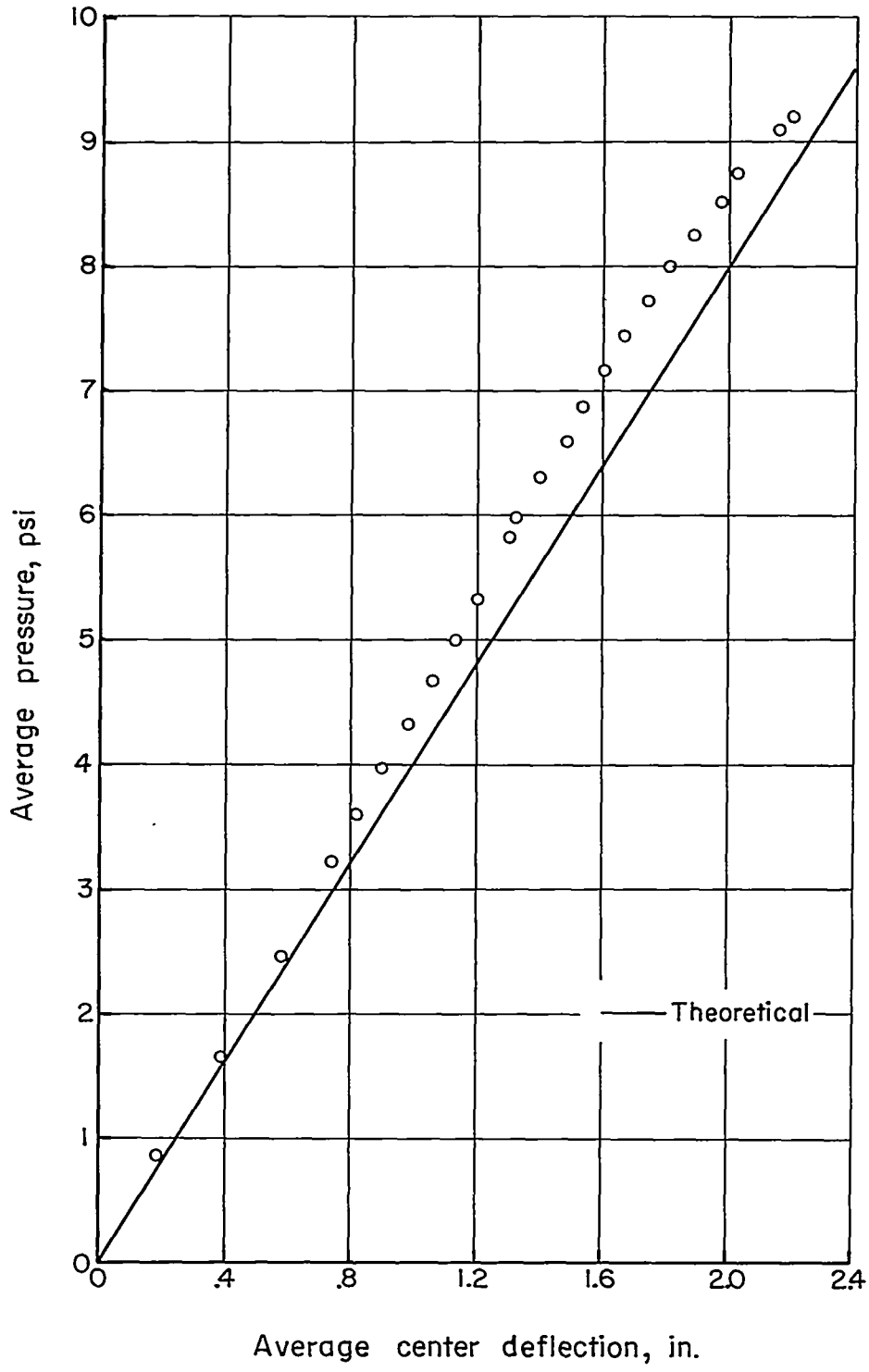

Figure 23.- Average lateral pressure against average center deflection for the lateral-load test of panel H 1/2 inch thick with faces of 0.032-inch aluminum-alloy sheet.

PANEL SIZE ?

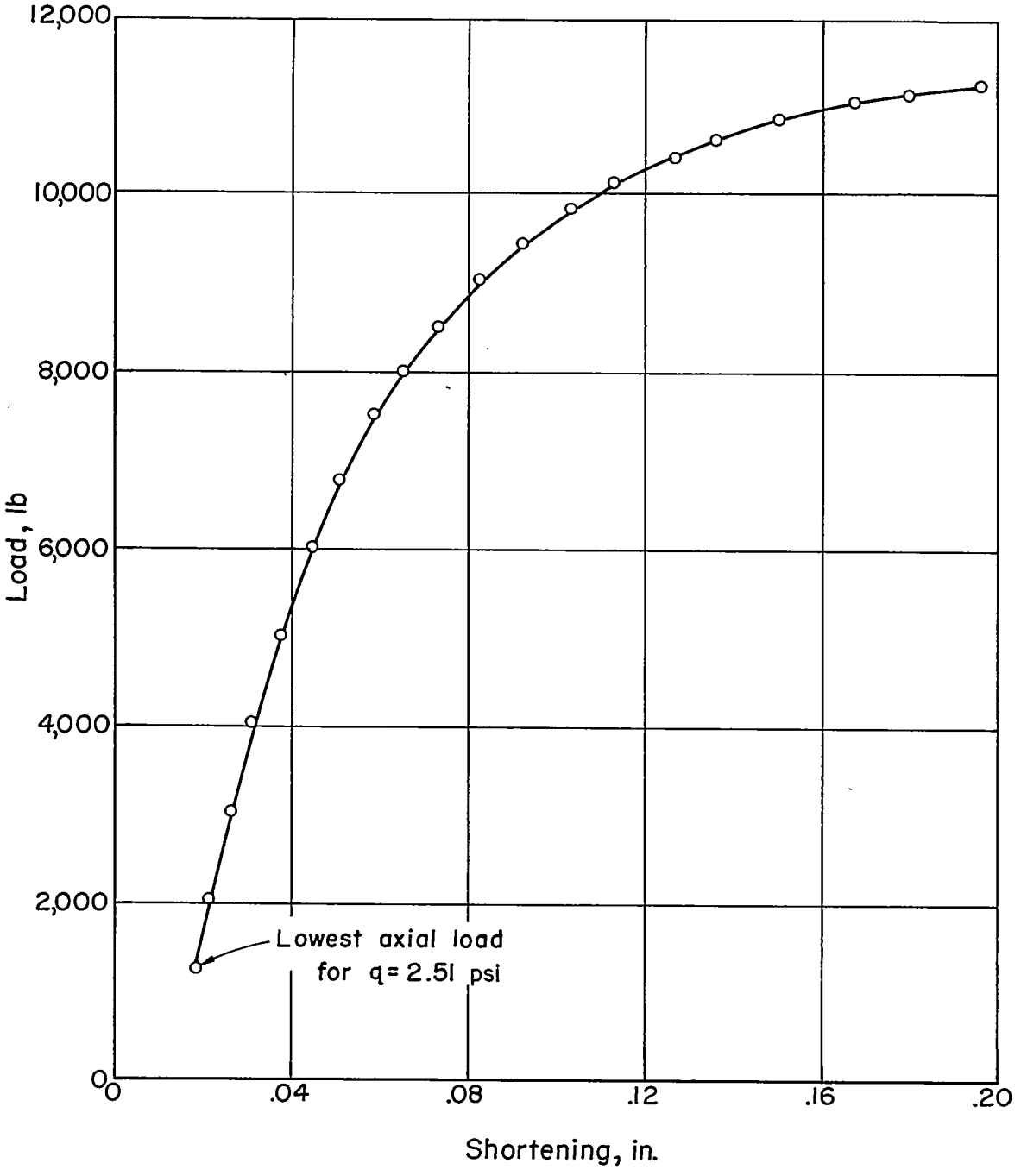

Figure 24.- Axial load against shortening for panel K. q = 2.51 psi.

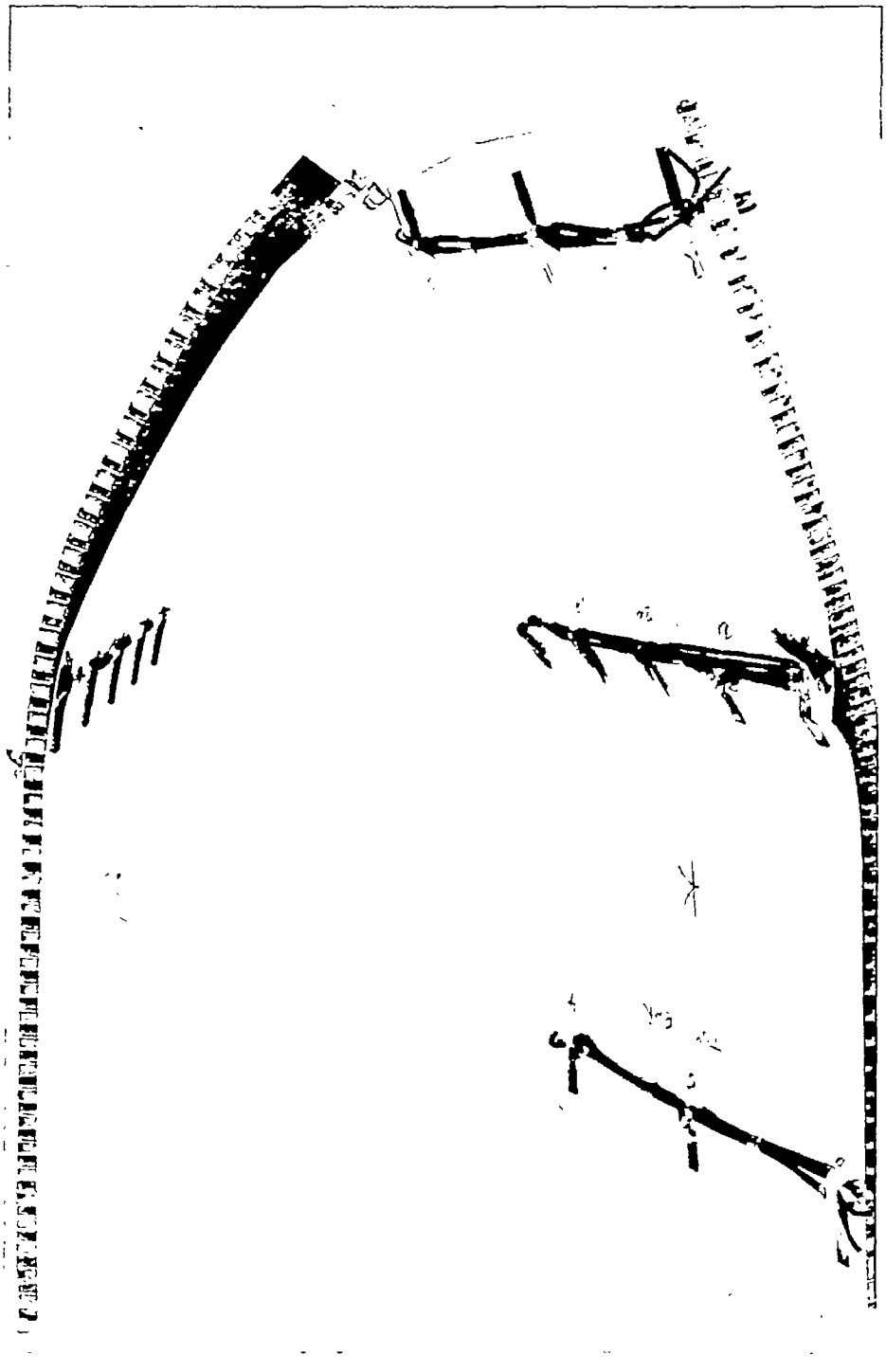

L-80275

(a) Lateral-pressure failure, panel H.

(b) Typical combined-loading failure, panel K.

Figure 25.- Panel failures.

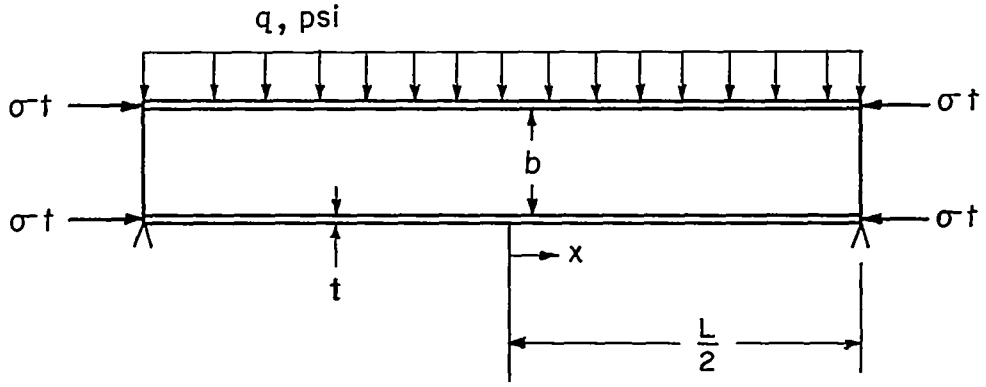

Figure 26.- Coordinates, dimensions, and loading of sandwich column used in theoretical analysis.

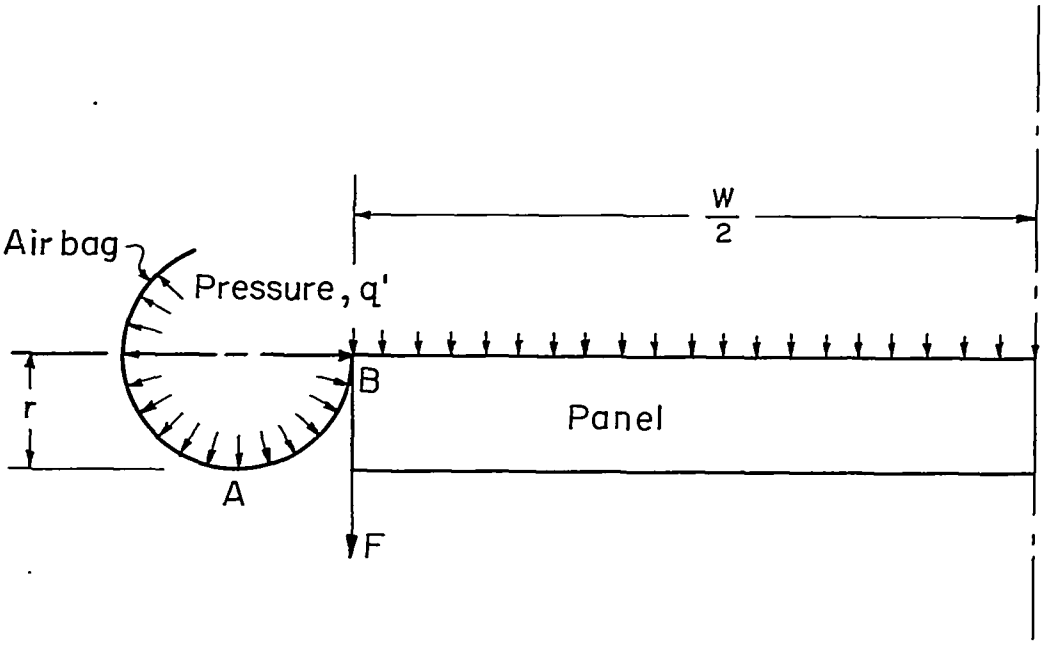

Figure 27.- Overlap of cloth air bag in combined-loading tests.

NACA-Langley - 12-15-53 - 1000